Published OnlineFirst March 17, 2011; DOI:10.1158/1078-0432.CCR-10-2798

added to each well, and the cells were incubated for 3 hours at 37°C before measurement of absorbance at 490 nm with a Multiskan Spectrum instrument (Thermo Labsystems).

RNA interference

Cells were plated at 50% to 60% confluence in 6-well plates or 25-cm^2 flasks and then incubated for 24 hours before transient transfection for the indicated times with siRNAs mixed with the Lipofectamine reagent (Invitrogen). The siRNAs specific for STAT3 mRNA (STAT3-1, 5′-UCAUUGACCUUGUGAAAAA-3′; STAT3-2, 5′-GCAAAAA-GUUUCCUACAAA-3′), ALK mRNA (ALK-1, 5′-ACACC-CAAAUUAAUACCAA-3′; ALK-2, 5′-UCAGCAAAUUCAA-CCACCA-3′), ERK mRNA (ERK-1, 5′-CAAGAGGAUUGAA-GUAGAA-3′; ERK-2, 5′-UCAGCCCCUUUGAGCACCA-3′), or BIM mRNA (BIM-1, 5′-GGAGGGUAUUUUUGAAUAA-3′; BIM-2, 5′-AGGAGGGUAUUUUUGAAUA-3′) as well as a nonspecific siRNA (5′-GUUGAGAGAUAUUAGAGUU-3′) were obtained from Nippon EGT. The cells were then subjected to immunoblot analysis or the annexin V–binding assay. All data presented were obtained with STAT3-1, ALK-1, ERK-1, or BIM-1 siRNAs, but similar results were obtained with STAT3-2, ALK-2, ERK-2, and BIM-2 siRNAs.

Annexin V–binding assay

Binding of annexin V to cells was measured with the use of an Annexin-V-FLUOS Staining kit (Roche). Cells were harvested by exposure to trypsin-EDTA, washed with PBS, and centrifuged at 200 × *g* for 5 minutes. The cell pellets were resuspended in 100 μL of Annexin-V-FLUOS labeling solution, incubated for 10 to 15 minutes at 15°C to 25°C, and then analyzed for fluorescence with a flow cytometer (FACSCalibur) and Cell Quest software (Becton Dickinson).

Statistical analysis

Quantitative data are presented as means ± SD and were analyzed by Student's 2-tailed *t* test. A value of $P < 0.05$ was considered statistically significant.

Results

Oncogenic EML4-ALK tyrosine kinase activates ERK and STAT3 signaling pathways

To study the function of oncogenic EML4-ALK, we established nontransformed mouse fibroblast (NIH 3T3) cells that either stably express EML4-ALK variant 1 or 3 (3T3/EAV1 and 3T3/EAV3 cells, respectively) or stably harbor the corresponding empty vector (3T3-Mock cells). Immunoblot analysis revealed that EML4-ALK variant 1 or 3 was detected with antibodies to ALK at positions corresponding to molecular sizes of about 120 and 90 kDa, respectively, in the transfected cells (Fig. 1A). The kinase activity of the EML4-ALK variants was activated as revealed by immunoblot

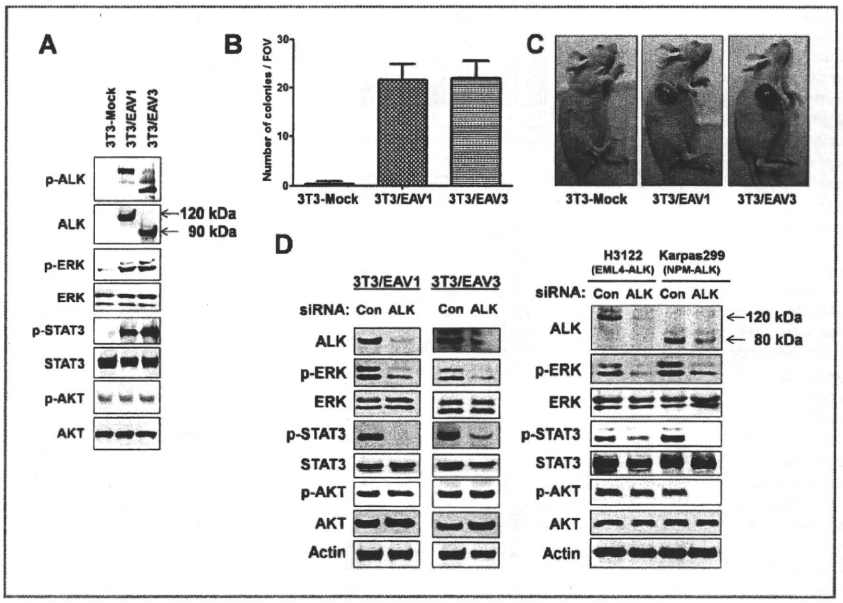

Figure 1. Effects of stable forced expression of EML4-ALK variant 1 or 3 on signaling pathways. A, the indicated stably transfected NIH 3T3 cell lines were lysed and subjected to immunoblot analysis with antibodies to the indicated proteins. B, the indicated cell lines were plated in semisolid medium supplemented with 10% FBS and incubated for 3 to 4 weeks, after which the cells were stained with 0.005% crystal violet and the number of colonies per field of view (FOV) was counted. Data are means ± SD from 3 independent experiments. C, cells (5×10^6) of the indicated lines were injected subcutaneously into the axilla of 5-week-old female athymic nude mice. At 18 days after the injection, the large tumors that formed at the injection site for 3T3/EAV1 or 3T3/EAV3 cells were photographed. Data are representative of results obtained with 5 mice per cell line. D, the indicated cell lines were transfected with nonspecific (Con) or ALK siRNAs for 48 hours, after which cell lysates were subjected to immunoblot analysis with antibodies to the indicated proteins.

Published OnlineFirst March 17, 2011; DOI:10.1158/1078-0432.CCR-10-2798

analysis with antibodies specific for the Tyr^{1608}-phosphorylated form of ALK. Consistent with previous observations (4, 15), the 3T3/EAV cells exhibited transforming activity both *in vitro* (Fig. 1B) and *in vivo* (Fig. 1C). We also found that phosphorylation of both the mitogen-activated protein kinase (MAPK) ERK and STAT3 was markedly increased in the cells expressing either variant of EML4-ALK compared with that in 3T3-Mock cells, whereas the phosphorylation level of the kinase AKT was not affected by expression of EML4-ALK (Fig. 1A). To exclude the possibility that these results were due to nonspecific effects of transfection, we depleted both 3T3/EAV1 and 3T3/EAV3 cells of EML4-ALK by RNA interference (RNAi) with ALK siRNA. The phosphorylation of both ERK and STAT3, but not that of AKT, was markedly suppressed by depletion of EML4-ALK (Fig. 1D). Moreover, similar depletion of endogenous EML4-ALK variant 1 in the lung cancer cell line H3122 resulted in marked inhibition of the phosphorylation of ERK and STAT3 without an effect on that of AKT (Fig. 1D). In contrast, the phosphorylation of ERK, STAT3, and AKT was inhibited by ALK siRNA in the NPM-ALK–positive lymphoma cell line Karpas299 (Fig. 1D), in which activation of the phosphoinositide 3-kinase (PI3K)-AKT signaling pathway has been shown to contribute to malignant transformation (22–25). Together, these data suggested that either variant 1 or 3 of EML4-ALK activates ERK and STAT3 signaling pathways but not the PI3K-AKT signaling pathway.

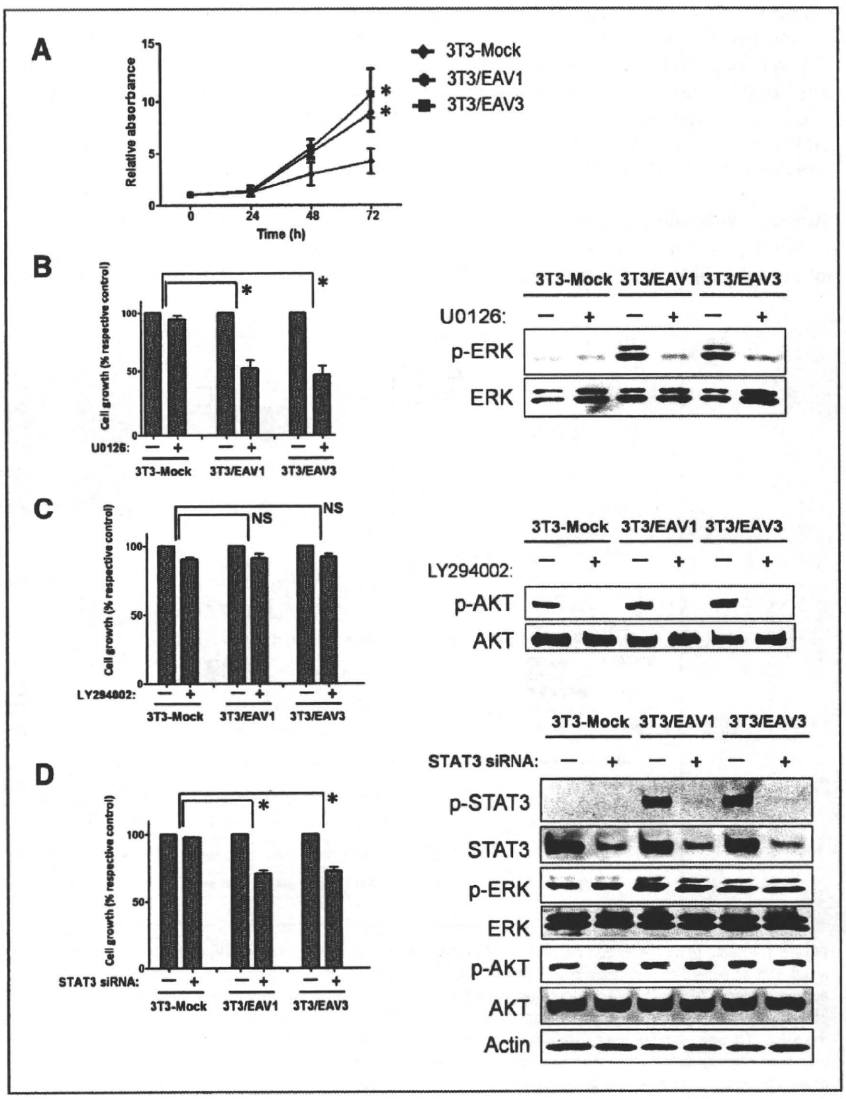

Figure 2. Effects of inhibition of ERK, PI3K, or STAT3 signaling on the growth of cells expressing EML4-ALK. A, the indicated cell lines were incubated in complete medium for the indicated times, after which cell viability was assessed as described in the "Materials and Methods" section. Data are expressed relative to the absorbance value for 3T3-Mock cells at time 0. B and C, cells were incubated in complete medium with or without 10 μmol/L U0126 (B) or 10 μmol/L LY294002 (C) for 72 or 24 hours, after which cell viability was assessed (left) or cell lysates were subjected to immunoblot analysis with antibodies to the indicated proteins (right), respectively. D, cells were transfected with nonspecific or STAT3 siRNAs for 72 or 48 hours, after which cell viability was assessed (left) or cell lysates were subjected to immunoblot analysis with antibodies to the indicated proteins (right), respectively. The abundance of β-actin was examined as a loading control. All quantitative data are means ± SD from 3 independent experiments. *, $P < 0.05$ versus the corresponding value for 3T3-Mock cells or for the indicated comparisons. NS, not significant.

Published OnlineFirst March 17, 2011; DOI:10.1158/1078-0432.CCR-10-2798

EML4-ALK promotes cell proliferation through ERK and STAT3 signaling pathways

We next examined the effect of EML4-ALK on cell proliferation. Both 3T3/EAV1 and 3T3/EAV3 cells proliferated significantly faster than did 3T3-Mock cells (Fig. 2A). To determine the role of intracellular signaling pathways in this action of EML4-ALK, we first examined the effects of chemical inhibitors. We found that U0126, an inhibitor of the ERK kinase MEK, had little effect on the growth of 3T3-Mock cells but that it significantly inhibited the proliferation of both 3T3/EAV1 and 3T3/EAV3 cells at a concentration (10 μmol/L) that resulted in marked inhibition of ERK phosphorylation (Fig. 2B). These data thus suggested that the MEK-ERK signaling pathway contributes to the regulation of cell proliferation by EML4-ALK. We also found that the specific PI3K inhibitor LY294002 had no significant effect on the growth of 3T3-Mock cells or on that of 3T3/EAV1 and 3T3/EAV3 cells at a concentration (10 μmol/L) at which the phosphorylation of AKT was largely abolished (Fig. 2C). To examine the effect of STAT3 inhibition on cell proliferation in cells expressing EML4-ALK, we transfected the cells with an siRNA specific for STAT3 mRNA. Transfection of 3T3-Mock, 3T3/EAV1, or 3T3/EAV3 cells with STAT3 siRNA resulted in marked depletion of STAT3 (Fig. 2D). Whereas such depletion of STAT3 did not affect the proliferation of 3T3-Mock cells, it significantly inhibited that of 3T3/EAV1 and 3T3/EAV3 cells (Fig. 2D). A

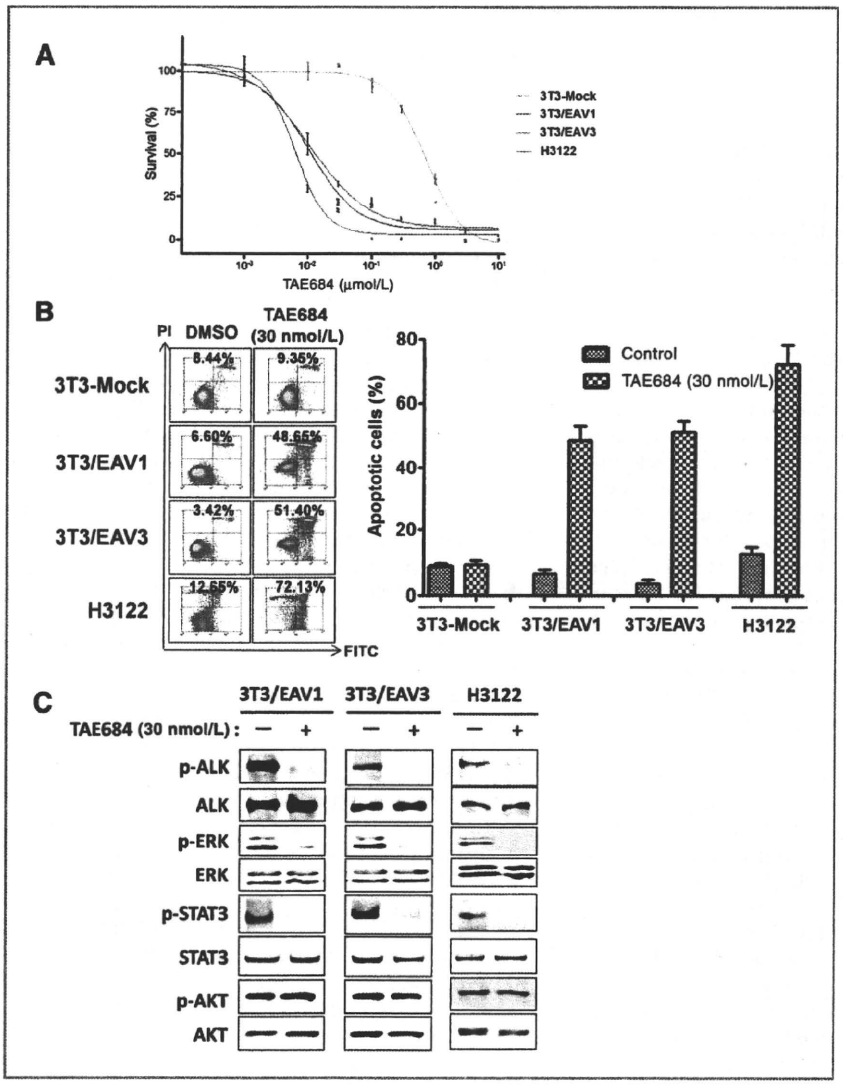

Figure 3. Effects of TAE684 on cell growth, apoptosis, and intracellular signaling in cells expressing EML4-ALK. A, the indicated cell lines were cultured for 72 hours in complete medium containing various concentrations of TAE684, after which cell viability was assessed. Data are expressed as percent survival and are means ± SD of triplicates from an experiment that was repeated a total of 3 times with similar results. B, cells were incubated for 48 hours in serum-free medium with 30 nmol/L TAE684 or 0.01% dimethyl sulfoxide (DMSO, vehicle control), after which the proportion of apoptotic cells was determined by staining with fluorescein isothiocyanate (FITC)-conjugated annexin V and propidium iodide (PI) followed by flow cytometry. Representative flow cytometric profiles, with the percentages of FITC-positive, PI-negative (apoptotic) cells indicated, are shown in the left. Quantitative data in the right are means ± SD of triplicates from an experiment that was repeated a total of 3 times with similar results. C, cells were incubated for 24 hours in serum-free medium with or without 30 nmol/L TAE684, after which cell lysates were subjected to immunoblot analysis with antibodies to the indicated proteins.

Published OnlineFirst March 17, 2011; DOI:10.1158/1078-0432.CCR-10-2798

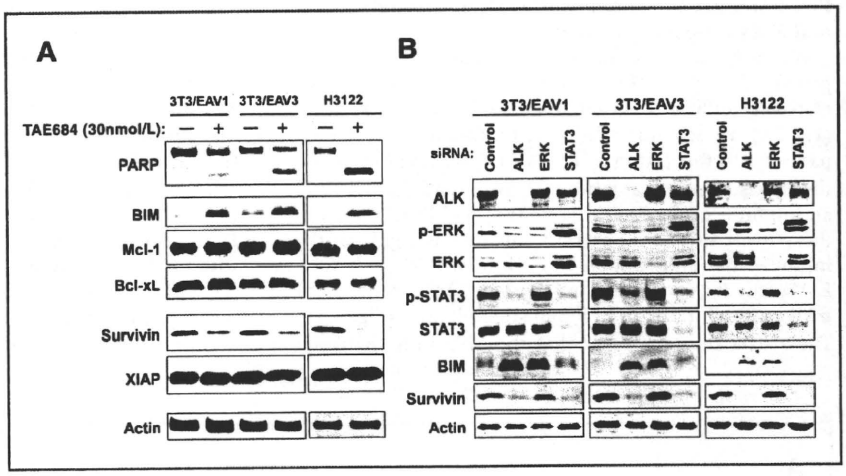

Figure 4. Effects of TAE684 on the expression of apoptosis-related proteins in cells expressing EML4-ALK. A, the indicated cell lines were incubated for 48 hours in serum-free medium with or without 30 nmol/L TAE684, after which cell lysates were subjected to immunoblot analysis with antibodies to the indicated proteins. B, 3T3/EAV1, 3T3/EAV3, or H3122 cells were transfected with nonspecific (control), ALK, ERK, or STAT3 siRNAs for 48 hours, after which cell lysates were subjected to immunoblot analysis with antibodies to the indicated proteins.

second siRNA targeted to a different region of STAT3 mRNA yielded similar results (data not shown). These observations thus suggested that EML4-ALK promotes cell proliferation through both MEK-ERK and STAT3 signaling pathways but not through the PI3K-AKT signaling pathway.

Effects of ALK inhibition on cell growth and intracellular signaling in EML4-ALK–positive lung cancer cells

To investigate the effects of inhibition of the kinase activity of ALK on cell growth and intracellular signaling in cells expressing EML4-ALK, we used TAE684, a selective and highly potent ALK inhibitor (26). The human lung cancer cell line H3122 expresses endogenous EML4-ALK variant 1 and its growth was found to be highly sensitive to TAE684 (Fig. 3A). Treatment with TAE684 also induced a large increase in the number of apoptotic H3122 cells, as revealed with an annexin V–binding assay (Fig. 3B). Consistent with these results, both 3T3/EAV1 and 3T3/EAV3 cells exhibited a sensitivity to TAE684 that was about 100 times as great as that of 3T3-Mock cells (Fig. 3A), and the level of apoptosis induced by this drug was markedly greater in both 3T3/EAV1 and 3T3/EAV3 cells than in 3T3-Mock cells (Fig. 3B). Immunoblot analysis revealed that TAE684 inhibited the phosphorylation of EML4-ALK in 3T3/EAV1, 3T3/EAV3, and H3122 cells at a concentration (30 nmol/L) at which it substantially inhibited the growth of these cells (Fig. 3C). We further found that TAE684 inhibited the activation of ERK and STAT3, without affecting that of AKT, in all 3 of these cell lines (Fig. 3C). These data thus suggested that the ALK inhibitor induced growth suppression and apoptosis in EML4-ALK–positive lung cancer cells, and that these effects were accompanied by inhibition of ERK and STAT3 signaling pathways but not by that of the PI3K-AKT signaling pathway.

Effects of ALK inhibition on the expression of apoptosis-related proteins in EML4-ALK–positive lung cancer cells

Given that TAE684 induced apoptosis in cells expressing EML4-ALK, we examined the effects of this drug on the expression of apoptosis-related proteins in such cells. TAE684 induced cleavage of PARP, a characteristic of apoptosis, in H3122 cells as well as in 3T3/EAV1 and 3T3/EAV3 cells (Fig. 4A). TAE684 also increased the abundance of BIM, a proapoptotic member of the Bcl-2 family of proteins, in cells expressing EML4-ALK, whereas the amounts of the Bcl-2 family members Mcl-1 and Bcl-xL remained unaffected (Fig. 4A). In contrast, TAE684 induced downregulation of the expression of survivin, a member of the IAP family, in cells expressing EML4-ALK, whereas the expression of XIAP, another IAP family member, remained unaffected (Fig. 4A). To investigate the possible roles of the ERK and STAT3 signaling pathways in the induction of BIM and downregulation of survivin by TAE684, we examined the effects of EML4-ALK, ERK, or STAT3 depletion by RNAi in 3T3/EAV1, 3T3/EAV3, and H3122 cells. Similar to the effects of TAE684 (Fig. 3C), depletion of EML4-ALK with an ALK siRNA resulted in inhibition of both ERK and STAT3 phosphorylation in all 3 cell lines (Fig. 4B). The amount of BIM was increased as a result of EML4-ALK or ERK depletion but was not affected by STAT3 depletion (Fig. 4B). In contrast, the expression of survivin was inhibited by depletion of EML4-AKT or STAT3 but not by that of ERK (Fig. 4B). Similar results were obtained with a second set of ALK, ERK, and STAT3 siRNAs targeted to different regions of the corresponding mRNAs (data not shown). These data thus suggested that ALK inhibition results in upregulation of BIM expression through inhibition of the ERK signaling pathway as well as in downregulation of survivin expression through inhibition of the STAT3 signaling pathway.

Published OnlineFirst March 17, 2011; DOI:10.1158/1078-0432.CCR-10-2798

Role of ERK-BIM and STAT3-survivin signaling pathways in TAE684-induced apoptosis in cells expressing EML4-ALK

To investigate further whether induction of BIM is related to TAE684-induced apoptosis, we transfected 3T3/EAV3 or H3122 cells with an siRNA specific for BIM mRNA. Such transfection largely blocked BIM induction by TAE684 (Fig. 5A). Staining with annexin V revealed that RNAi-mediated attenuation of BIM induction resulted in significant inhibition of TAE684-induced apoptosis in both cell lines (Fig. 5A), implicating upregulation of BIM expression in the induction of apoptosis by TAE684 in EML4-ALK–positive cells. We obtained similar results with a second siRNA targeted to a different sequence within BIM mRNA (data not shown). Given that TAE684 inhibited STAT3-survivin signaling in cells expressing EML4-ALK, we next investigated the contribution of such signaling to TAE684-induced apoptosis by transfecting 3T3/EAV3 or H3122 cells with an expression vector encoding a FLAG epitope–tagged constitutively active (CA) form of human STAT3. Expression of CA-STAT3 increased the abundance of survivin (Fig. 5B), consistent with the notion that survivin expression is upregulated by activation of STAT3 signaling. Furthermore, expression of CA-STAT3 inhibited the downregulation of survivin induced by TAE684, without affecting BIM induction (Fig. 5B), and it significantly inhibited TAE684-induced apoptosis (Fig. 5B). These data suggested that inhibition of the STAT3 signaling pathway contributes to TAE684-induced apoptosis in EML4-ALK–positive cells. To confirm that TAE684-induced apoptosis mediated by STAT3 inhibition was attributable to downregulation of survivin expression, we transfected 3T3/EAV3 or H3122 cells with an expression vector for human survivin. Survivin overexpression resulted in substantial inhibition of the TAE684-induced downregulation of survivin in both 3T3/EAV3 and H3122 cells (Fig. 5C), and this effect was associated with significant inhibition

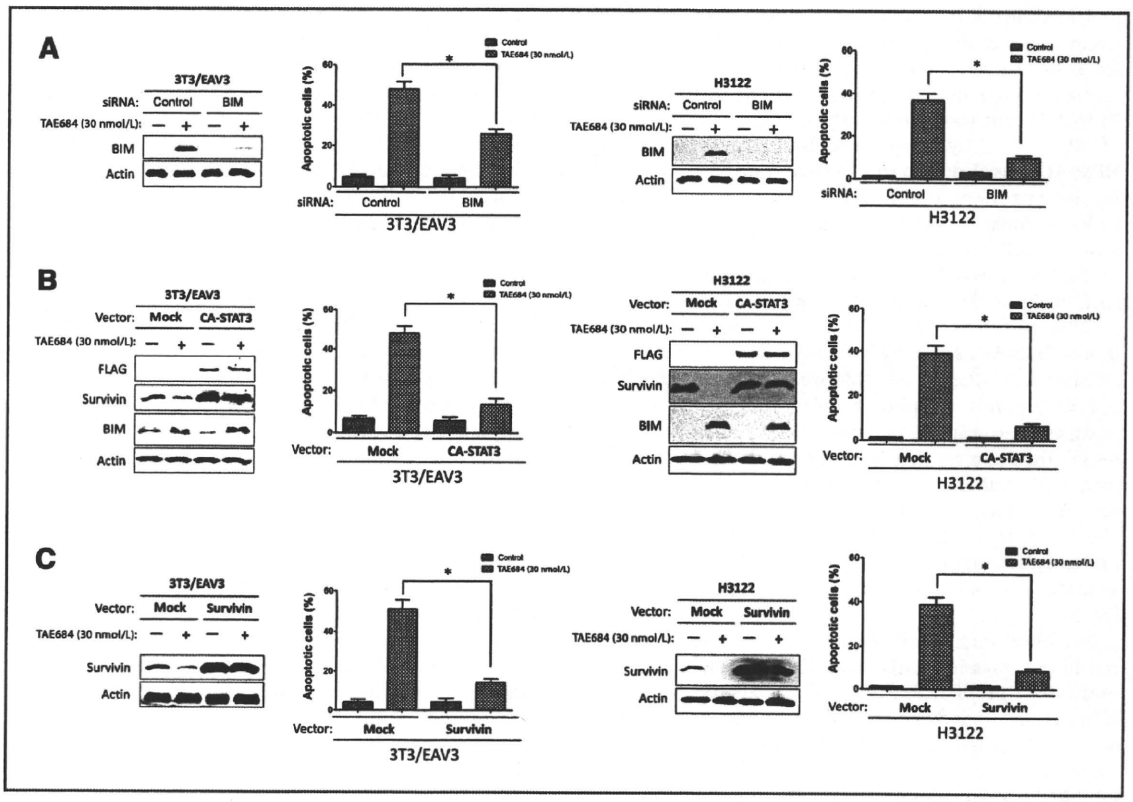

Figure 5. Effects of BIM depletion as well as forced expression of CA-STAT3 and survivin on apoptosis induced by TAE684 in 3T3/EAV3 or H3122 cells. A, cells were transfected with nonspecific (control) or BIM siRNAs for 24 hours and then incubated in complete medium with 30 nmol/L TAE684 or DMSO vehicle for 48 hours, after which cells either were lysed and subjected to immunoblot analysis with antibodies to the indicated proteins or were evaluated for apoptosis by staining with annexin V and PI followed by flow cytometry. B, cells were transfected with an expression vector for FLAG-tagged CA-STAT3 or with the corresponding empty vector for 24 hours and were then incubated with or without 30 nmol/L TAE684 for 48 hours and analyzed as in A. C, cells were transfected with an expression vector for survivin or with the corresponding empty vector for 24 hours and were then incubated with or without 30 nmol/L TAE684 for 48 hours and analyzed as in A. All quantitative data are means ± SD from at least 3 independent experiments. *, $P < 0.05$ for the indicated comparisons.

Published OnlineFirst March 17, 2011; DOI:10.1158/1078-0432.CCR-10-2798

of TAE684-induced apoptosis (Fig. 5C). These results thus suggested that inhibition of STAT3-survivin signaling by TAE684 contributes substantially to the induction of apoptosis by this drug. Collectively, our results thus suggested that inhibition of both the ERK-BIM and STAT3-survivin signaling pathways contributes to the induction of apoptosis associated with ALK inhibition in EML4-ALK–positive lung cancer cells.

Discussion

EML4-ALK was only recently identified as a transforming fusion gene in NSCLC (4). Although EML4-ALK was shown to possess marked oncogenic activity both *in vitro* and *in vivo* (4, 15), the signaling pathways underlying malignant transformation by the fusion protein have remained unclear. We have now shown that phosphorylation of both ERK and STAT3 was similarly and markedly increased in NIH 3T3 cells by forced expression of either variant 1 or variant 3 of EML4-ALK, whereas phosphorylation of AKT remained unaffected. Similar effects were observed in different clones of these cells stably transfected with a vector for either variant of EML4-ALK (data not shown). We further showed that the growth of both 3T3/EAV1 and 3T3/EAV3 cells was significantly attenuated by inhibition of ERK or STAT3 signaling but not by that of PI3K signaling. NPM-ALK has also been shown to activate ERK and STAT3 signaling pathways (6, 27–33), both of which are thought to be essential downstream mediators of the oncogenic action of NPM-ALK. In the present study, we found that ALK siRNA markedly abrogated the phosphorylation of AKT in the NPM-ALK–positive lymphoma cell line Karpas299, consistent with previous results implicating activation of PI3K-AKT signaling in malignant transformation by NPM-ALK (22–25). In contrast, we found that ALK siRNA did not suppress AKT phosphorylation in the EML4-ALK–positive lung cancer cell line H3122. Together, our results thus suggest that both ERK and STAT3 signaling pathways, rather than the PI3K signaling pathway, are the principal downstream pathways activated by EML4-ALK in lung cancer cells. Oncogenic ALK fusion proteins therefore may activate downstream pathways in a manner dependent on the fusion partner (Supplementary Fig. S1).

Preclinical studies have shown that treatment of NSCLC cell lines expressing EML4-ALK with ALK inhibitors suppresses cell proliferation and induces apoptosis (9, 34), although the underlying mechanisms of these effects were not well characterized. We have now shown that TAE684, a specific inhibitor of the kinase activity of ALK, significantly inhibited the phosphorylation of ERK and STAT3, but not that of AKT, in EML4-ALK–positive lung cancer cells, supporting the notion that ERK and STAT3 signaling pathways function downstream of EML4-ALK. BIM is a key proapoptotic member of the Bcl-2 family of proteins and initiates apoptosis signaling by binding to and antagonizing the function of prosurvival members of the Bcl-2 family (35). We found that TAE684 induced upregulation of BIM in EML4-ALK–positive lung cancer cells. With the use of RNAi-mediated depletion of ERK, we also found that BIM expression is regulated by the ERK signaling pathway. We further showed that knockdown of BIM by RNAi resulted in significant inhibition of TAE684-induced apoptosis in EML4-ALK–positive cells, suggesting that BIM induction mediated by inhibition of the ERK pathway plays a pivotal role in ALK inhibitor–induced apoptosis in EML4-ALK–positive lung cancer cells. These findings are consistent with the previous observation that inhibition of the ERK pathway contributes to EGFR-TKI–induced BIM upregulation, which is essential for the induction of apoptosis by these agents, in *EGFR* mutation–positive NSCLC cells (36–38).

Survivin is a member of the IAP family and protects against apoptosis by either directly or indirectly inhibiting the activation of effector caspases (39). We have now shown that TAE684 inhibited the expression of survivin in EML4-ALK–positive lung cancer cells. Furthermore, depletion of STAT3 resulted in downregulation of survivin expression, whereas expression of a constitutively active form of STAT3 resulted in upregulation of survivin expression. These data indicate that expression of survivin is regulated primarily through the STAT3 signaling pathway, consistent with the results of a previous study (40). We further found that expression of CA-STAT3 blocked the TAE684-induced downregulation of survivin, indicating that ALK inhibition results in survivin downregulation through inhibition of the STAT3 signaling pathway. Forced expression of either CA-STAT3 or survivin attenuated TAE684-induced apoptosis in 3T3/EAV3 or H3122 cells, suggesting that inhibition of STAT3-survivin signaling contributes to ALK inhibitor–induced apoptosis in EML4-ALK–positive lung cancer cells. Our present data thus suggest that ALK inhibitor–induced apoptosis is mediated both by upregulation of BIM through inhibition of the ERK pathway and by downregulation of survivin through inhibition of the STAT3 pathway in EML4-ALK–positive lung cancer cells.

In conclusion, our results have identified both ERK and STAT3 signaling pathways as key mediators of the transforming activity of EML4-ALK in lung cancer cells positive for this fusion protein. We further demonstrated that inhibition of both ERK-BIM and STAT3-survivin signaling pathways is responsible for ALK inhibitor–induced apoptosis in these cells. Our results thus provide a basis for the further development of ALK-targeted therapy in EML4-ALK–positive lung cancer patients.

Disclosure of Potential Conflicts of Interest

No potential conflicts of interest were disclosed.

The costs of publication of this article were defrayed in part by the payment of page charges. This article must therefore be hereby marked *advertisement* in accordance with 18 U.S.C. Section 1734 solely to indicate this fact.

Received October 19, 2010; revised January 20, 2011; accepted February 10, 2011; published OnlineFirst March 17, 2011.

Published OnlineFirst March 17, 2011; DOI:10.1158/1078-0432.CCR-10-2798

References

1. Lynch TJ, Bell DW, Sordella R, Gurubhagavatula S, Okimoto RA, Brannigan BW, et al. Activating mutations in the epidermal growth factor receptor underlying responsiveness of non-small-cell lung cancer to gefitinib. N Engl J Med 2004;350:2129–39.
2. Paez JG, Janne PA, Lee JC, Tracy S, Greulich H, Gabriel S, et al. EGFR mutations in lung cancer: correlation with clinical response to gefitinib therapy. Science 2004;304:1497–500.
3. Pao W, Miller V, Zakowski M, Doherty J, Politi K, Sarkaria I, et al. EGF receptor gene mutations are common in lung cancers from "never smokers" and are associated with sensitivity of tumors to gefitinib and erlotinib. Proc Natl Acad Sci U S A 2004;101:13306–11.
4. Soda M, Choi YL, Enomoto M, Takada S, Yamashita Y, Ishikawa S, et al. Identification of the transforming EML4-ALK fusion gene in non-small-cell lung cancer. Nature 2007;448:561–6.
5. Morris SW, Kirstein MN, Valentine MB, Dittmer KG, Shapiro DN, Saltman DL, et al. Fusion of a kinase gene, ALK, to a nucleolar protein gene, NPM, in non-Hodgkin's lymphoma. Science 1994;263:1281–4.
6. Fujimoto J, Shiota M, Iwahara T, Seki N, Satoh H, Mori S, et al. Characterization of the transforming activity of p80, a hyperphosphorylated protein in a Ki-1 lymphoma cell line with chromosomal translocation t(2;5). Proc Natl Acad Sci U S A 1996;93:4181–6.
7. Inamura K, Takeuchi K, Togashi Y, Nomura K, Ninomiya H, Okui M, et al. EML4-ALK fusion is linked to histological characteristics in a subset of lung cancers. J Thorac Oncol 2008;3:13–7.
8. Inamura K, Takeuchi K, Togashi Y, Hatano S, Ninomiya H, Motoi N, et al. EML4-ALK lung cancers are characterized by rare other mutations, a TTF-1 cell lineage, an acinar histology, and young onset. Mod Pathol 2009;22:508–15.
9. Koivunen JP, Mermel C, Zejnullahu K, Murphy C, Lifshits E, Holmes AJ, et al. EML4-ALK fusion gene and efficacy of an ALK kinase inhibitor in lung cancer. Clin Cancer Res 2008;14:4275–83.
10. Shinmura K, Kageyama S, Tao H, Bunai T, Suzuki M, Kamo T, et al. EML4-ALK fusion transcripts, but no NPM-, TPM3-, CLTC-, ATIC-, or TFG-ALK fusion transcripts, in non-small cell lung carcinomas. Lung Cancer 2008;61:163–9.
11. Martelli MP, Sozzi G, Hernandez L, Pettirossi V, Navarro A, Conte D, et al. EML4-ALK rearrangement in non-small cell lung cancer and non-tumor lung tissues. Am J Pathol 2009;174:661–70.
12. Shaw AT, Yeap BY, Mino-Kenudson M, Digumarthy SR, Costa DB, Heist RS, et al. Clinical features and outcome of patients with non-small-cell lung cancer who harbor EML4-ALK. J Clin Oncol 2009;27:4247–53.
13. Wong DW, Leung EL, So KK, Tam IY, Sihoe AD, Cheng LC, et al. The EML4-ALK fusion gene is involved in various histologic types of lung cancers from nonsmokers with wild-type EGFR and KRAS. Cancer 2009;115:1723–33.
14. Sasaki T, Rodig SJ, Chirieac LR, Janne PA. The biology and treatment of EML4-ALK non-small cell lung cancer. Eur J Cancer 2010;46:1773–80.
15. Choi YL, Takeuchi K, Soda M, Inamura K, Togashi Y, Hatano S, et al. Identification of novel isoforms of the EML4-ALK transforming gene in non-small cell lung cancer. Cancer Res 2008;68:4971–6.
16. Soda M, Takada S, Takeuchi K, Choi YL, Enomoto M, Ueno T, et al. A mouse model for EML4-ALK-positive lung cancer. Proc Natl Acad Sci U S A 2008;105:19893–7.
17. Kwak EL, Bang YJ, Camidge DR, Shaw AT, Solomon B, Maki RG, et al. Anaplastic lymphoma kinase inhibition in non-small-cell lung cancer. N Engl J Med 2011;363:1693–703.
18. Bromberg JF, Wrzeszczynska MH, Devgan G, Zhao Y, Pestell RG, Albanese C, et al. Stat3 as an oncogene. Cell 1999;98:295–303.
19. Okamoto K, Okamoto I, Okamoto W, Tanaka K, Takezawa K, Kuwata K, et al. Role of survivin in EGFR tyrosine kinase inhibitor-induced apoptosis in EGFR mutation-positive non-small cell lung cancer. Cancer Res 2010;70:10402–10.
20. Okamoto W, Okamoto I, Tanaka K, Hatashita E, Yamada Y, Kuwata K, et al. TAK-701, a humanized monoclonal antibody to HGF, reverses gefitinib resistance induced by tumor-derived HGF in non-small cell lung cancer with an EGFR mutation. Mol Cancer Ther 2010;10:2785–92.
21. Tanaka K, Arao T, Maegawa M, Matsumoto K, Kaneda H, Kudo K, et al. SRPX2 is overexpressed in gastric cancer and promotes cellular migration and adhesion. Int J Cancer 2009;124:1072–80.
22. Bai RY, Ouyang T, Miething C, Morris SW, Peschel C, Duyster J. Nucleophosmin-anaplastic lymphoma kinase associated with anaplastic large-cell lymphoma activates the phosphatidylinositol 3-kinase/Akt antiapoptotic signaling pathway. Blood 2000;96:4319–27.
23. Polgar D, Leisser C, Maier S, Strasser S, Ruger B, Dettke M, et al. Truncated ALK derived from chromosomal translocation t(2;5)(p23;q35) binds to the SH3 domain of p85-PI3K. Mutat Res 2005;570:9–15.
24. Slupianek A, Nieborowska-Skorska M, Hoser G, Morrione A, Majewski M, Xue L, et al. Role of phosphatidylinositol 3-kinase-Akt pathway in nucleophosmin/anaplastic lymphoma kinase-mediated lymphomagenesis. Cancer Res 2001;61:2194–9.
25. Rassidakis GZ, Feretzaki M, Atwell C, Grammatikakis I, Lin Q, Lai R, et al. Inhibition of Akt increases p27Kip1 levels and induces cell cycle arrest in anaplastic large cell lymphoma. Blood 2005;105:827–9.
26. Galkin AV, Melnick JS, Kim S, Hood TL, Li N, Li L, et al. Identification of NVP-TAE684, a potent, selective, and efficacious inhibitor of NPM-ALK. Proc Natl Acad Sci U S A 2007;104:270–5.
27. Crockett DK, Lin Z, Elenitoba-Johnson KS, Lim MS. Identification of NPM-ALK interacting proteins by tandem mass spectrometry. Oncogene 2004;23:2617–29.
28. Marzec M, Kasprzycka M, Liu X, Raghunath PN, Wlodarski P, Wasik MA. Oncogenic tyrosine kinase NPM/ALK induces activation of the MEK/ERK signaling pathway independently of c-Raf. Oncogene 2007;26:813–21.
29. Amin HM, McDonnell TJ, Ma Y, Lin Q, Fujio Y, Kunisada K, et al. Selective inhibition of STAT3 induces apoptosis and G(1) cell cycle arrest in ALK-positive anaplastic large cell lymphoma. Oncogene 2004;23:5426–34.
30. Zamo A, Chiarle R, Piva R, Howes J, Fan Y, Chilosi M, et al. Anaplastic lymphoma kinase (ALK) activates Stat3 and protects hematopoietic cells from cell death. Oncogene 2002;21:1038–47.
31. Shi X, Franko B, Frantz C, Amin HM, Lai R. JSI-124 (cucurbitacin I) inhibits Janus kinase-3/signal transducer and activator of transcription-3 signalling, downregulates nucleophosmin-anaplastic lymphoma kinase (ALK), and induces apoptosis in ALK-positive anaplastic large cell lymphoma cells. Br J Haematol 2006;135:26–32.
32. Han Y, Amin HM, Franko B, Frantz C, Shi X, Lai R. Loss of SHP1 enhances JAK3/STAT3 signaling and decreases proteosome degradation of JAK3 and NPM-ALK in ALK +anaplastic large-cell lymphoma. Blood 2006;108:2796–803.
33. Chiarle R, Simmons WJ, Cai H, Dhall G, Zamo A, Raz R, et al. Stat3 is required for ALK-mediated lymphomagenesis and provides a possible therapeutic target. Nat Med 2005;11:623–9.
34. McDermott U, Iafrate AJ, Gray NS, Shioda T, Classon M, Maheswaran S, et al. Genomic alterations of anaplastic lymphoma kinase may sensitize tumors to anaplastic lymphoma kinase inhibitors. Cancer Res 2008;68:3389–95.
35. Chen L, Willis SN, Wei A, Smith BJ, Fletcher JI, Hinds MG, et al. Differential targeting of prosurvival Bcl-2 proteins by their BH3-only ligands allows complementary apoptotic function. Mol Cell 2005;17:393–403.
36. Costa DB, Halmos B, Kumar A, Schumer ST, Huberman MS, Boggon TJ, et al. BIM mediates EGFR tyrosine kinase inhibitor-induced apoptosis in lung cancers with oncogenic EGFR mutations. PLoS Med 2007;4:1669–79; discussion 1680.
37. Cragg MS, Kuroda J, Puthalakath H, Huang DC, Strasser A. Gefitinib-induced killing of NSCLC cell lines expressing mutant EGFR requires BIM and can be enhanced by BH3 mimetics. PLoS Med 2007;4:1681–89; discussion 1690.
38. Gong Y, Somwar R, Politi K, Balak M, Chmielecki J, Jiang X, et al. Induction of BIM is essential for apoptosis triggered by EGFR kinase inhibitors in mutant EGFR-dependent lung adenocarcinomas. PLoS Med 2007;4:e294.
39. Hengartner MO. The biochemistry of apoptosis. Nature 2000;407:770–6.
40. Aoki Y, Feldman GM, Tosato G. Inhibition of STAT3 signaling induces apoptosis and decreases survivin expression in primary effusion lymphoma. Blood 2003;101:1535–42.

Oncogene (2011) 1–10

www.nature.com/onc

ORIGINAL ARTICLE

Roles of BIM induction and survivin downregulation in lapatinib-induced apoptosis in breast cancer cells with *HER2* amplification

J Tanizaki[1], I Okamoto[1], S Fumita[1], W Okamoto[1], K Nishio[2] and K Nakagawa[1]

[1]*Department of Medical Oncology, Kinki University Faculty of Medicine, 377-2 Ohno-higashi, Osaka-Sayama, Osaka, Japan and* [2]*Department of Genome Biology, Kinki University Faculty of Medicine, 377-2 Ohno-higashi, Osaka-Sayama, Osaka, Japan*

Lapatinib, a dual tyrosine kinase inhibitor of the epidermal growth factor receptor and human epidermal growth factor receptor 2 (HER2), is clinically active in patients with breast cancer positive for *HER2* amplification. The mechanism of this anti-tumor action has remained unclear, however. We have now investigated the effects of lapatinib in *HER2* amplification-positive breast cancer cells with or without an activating *PIK3CA* mutation. Lapatinib induced apoptosis in association with upregulation of the pro-apoptotic protein Bcl-2 interacting mediator of cell death (BIM) through inhibition of the MEK-ERK signaling pathway in breast cancer cells with *HER2* amplification. RNA interference (RNAi)-mediated depletion of BIM inhibited lapatinib-induced apoptosis, implicating BIM induction in this process. The pro-apoptotic effect of lapatinib was less pronounced in cells with a *PIK3CA* mutation than in those without one. Lapatinib failed to inhibit AKT phosphorylation in *PIK3CA* mutant cells, likely because of hyperactivation of the phosphatidylinositol 3-kinase (PI3K) signaling pathway by the mutation. Depletion of PIK3CA (a catalytic subunit of PI3K) revealed that survivin expression is regulated by the PI3K pathway in these cells, suggesting that insufficient inhibition of PI3K-survivin signaling is responsible for the limited pro-apoptotic effect of lapatinib in *HER2* amplification-positive cells with a *PIK3CA* mutation. Consistent with this notion, depletion of survivin by RNAi or treatment with a PI3K inhibitor markedly increased the level of apoptosis in *PIK3CA* mutant cells treated with lapatinib. Our results thus suggest that inhibition of both PI3K-survivin and MEK-ERK-BIM pathways is required for effective induction of apoptosis in breast cancer cells with *HER2* amplification.
Oncogene advance online publication, 18 April 2011; doi:10.1038/onc.2011.111

Keywords: BIM; survivin; *HER2* amplification; *PIK3CA* mutation; apoptosis; breast cancer

Correspondence: Dr I Okamoto, Department of Medical Oncology, Kinki University Faculty of Medicine, 377-2 Ohno-higashi, Osaka-Sayama, Osaka, Japan.
E-mail: chi-okamoto@dotd.med.kindai.ac.jp
Received 3 October 2010; revised 17 February 2011; accepted 1 March 2011

Introduction

Breast cancer is the leading cause of cancer death among women worldwide. Amplification of the human epidermal growth factor receptor 2 (*HER2*) gene occurs in 25–30% of breast cancers (Slamon *et al.*, 1987, 1989), and HER2 is thus an attractive target for the development of therapeutic drugs. Lapatinib, a dual tyrosine kinase inhibitor of HER2 and the epidermal growth factor receptor (EGFR), has shown anti-tumor activity for breast cancer with *HER2* amplification in pre-clinical and clinical studies (Geyer *et al.*, 2006; Konecny *et al.*, 2006; Gomez *et al.*, 2008). Although lapatinib improved the overall outcome for such patients, not all patients were benefited from the treatment. Characterization of the molecular basis of the response to lapatinib will thus be important to maximize the clinical efficacy of this drug.

Mutations in *PIK3CA*, which encodes the p110α catalytic subunit of phosphatidylinositol 3-kinase (PI3K), have been identified in 8–40% of breast cancers (Samuels *et al.*, 2004; Saal *et al.*, 2005; Berns *et al.*, 2007). Although a positive correlation between HER2 overexpression and the presence of *PIK3CA* mutations has been described (Saal *et al.*, 2005), the relation between the efficacy of lapatinib and such mutations has remained unclear (Eichhorn *et al.*, 2008; Toi *et al.*, 2009; Kataoka *et al.*, 2010). We have therefore now investigated the effects of lapatinib in *HER2* amplification-positive breast cancer cells with or without an activating *PIK3CA* mutation, and we further examined the mechanism responsible for the induction of apoptosis in these cells.

Results

Lapatinib inhibits cell proliferation and induces apoptosis in breast cancer cells with HER2 *amplification*

We first examined the effect of lapatinib on the proliferation *in vitro* of breast cancer cells positive or negative for *HER2* amplification (Figure 1a). All six cell lines with *HER2* amplification, including SK-BR3, ZR-75-30, BT-474, MB-361, MB-453 and HCC1954, were sensitive to lapatinib, with median inhibitory concentration (IC_{50}) values ranging from 0.05 to 0.80 μM, which are within the clinically achievable concentration range

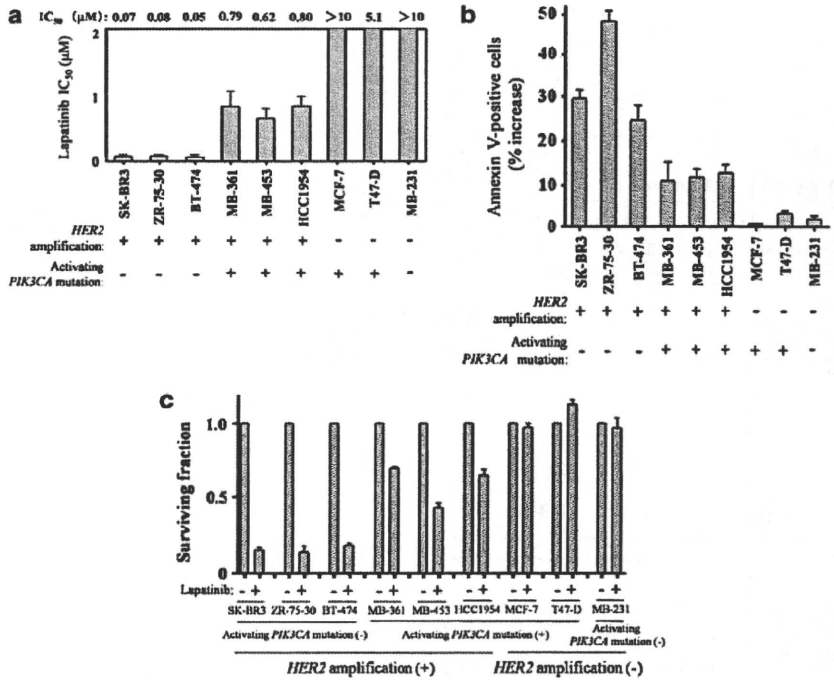

Figure 1 Effects of lapatinib on cell proliferation and apoptosis in breast cancer cells classified according to *HER2* and *PIK3CA* status. (**a**) The indicated cell lines were cultured for 72 h in complete culture medium containing various concentrations of lapatinib, after which the number of viable cells was determined and the IC_{50} value of lapatinib for inhibition of cell proliferation was calculated. (**b**) The indicated cell lines were incubated for 72 h with lapatinib (1 μM), after which the number of apoptotic cells was determined by staining with annexin V and propidium iodide followed by flow cytometry. The percentage increase in the number of apoptotic cells relative to the corresponding value for cells incubated without lapatinib is shown. (**c**) The indicated cell lines were cultured for 14 days in the presence of lapatinib (1 μM) before determination of the number of colonies for calculation of the surviving fraction relative to that of control cells incubated without lapatinib. All data are means ± s.e. from three independent experiments.

for this drug (LoRusso *et al*., 2008; Burris *et al*., 2009). Among these *HER2* amplification-positive cells, those with an activating *PIK3CA* mutation (MB-361, MB-453 and HCC1954) were less sensitive to lapatinib than were those without such a mutation (SK-BR3, ZR-75-30 and BT-474). Cell lines negative for *HER2* amplification, including MCF-7, T47-D and MB-231, were resistant to lapatinib, with IC_{50} values of >5.0 μM.

We next examined the effect of lapatinib on apoptosis in these various breast cancer cell lines (Figure 1b). An annexin V binding assay showed that lapatinib (1 μM) induced apoptosis in all *HER2* amplification-positive cells, but was largely without effect in amplification-negative cells. Consistent with the IC_{50} values for the anti-proliferative effect of the drug, the extent of lapatinib-induced apoptosis was less pronounced in *HER2* amplification-positive cells with an activating *PIK3CA* mutation than in those without such a mutation. We further examined the effect of lapatinib on clonogenic survival of breast cancer cells. Again, lapatinib greatly reduced the clonogenicity of *HER2* amplification-positive cells without a *PIK3CA* mutation, whereas the reduction in the number of clones was less marked for those with a *PIK3CA* mutation (Figure 1c). These data thus revealed that lapatinib exerts anti-proliferative and anti-survival effects in cells positive for *HER2* amplification, but the extent of these effects is smaller for such cells with a *PIK3CA* mutation than for those without this genetic change.

Differential effect of lapatinib on AKT signaling in HER2 *amplification-positive breast cancer cells with or without an activating* PIK3CA *mutation*

We examined the effects of lapatinib on the AKT and ERK (extracellular signal-regulated kinase) signaling pathways in breast cancer cell lines (Figure 2a). Immunoblot analysis showed that phosphorylation of both AKT and ERK was markedly inhibited by lapatinib in *HER2* amplification-positive cells without an activating *PIK3CA* mutation. In *HER2* amplification-positive cells harboring a *PIK3CA* mutation, however, lapatinib inhibited the phosphorylation of ERK but had little effect on that of AKT. Lapatinib showed little effect on the phosphorylation of AKT or ERK in *HER2* amplification-negative cells. These data thus revealed that, whereas lapatinib inhibited the phosphorylation of ERK in all *HER2* amplification-positive cells, its effect on that of AKT was dependent on *PIK3CA* mutational status.

Effects of lapatinib on apoptosis-related proteins in HER2 *amplification-positive breast cancer cells with or without an activating* PIK3CA *mutation*

Given that lapatinib induced apoptosis in cells with *HER2* amplification, we examined its effects on apoptosis-related proteins in these cells (Figure 2b). Immunoblot analysis revealed that lapatinib upregulated the expression of Bcl-2 interacting mediator of cell death (BIM), a pro-apoptotic

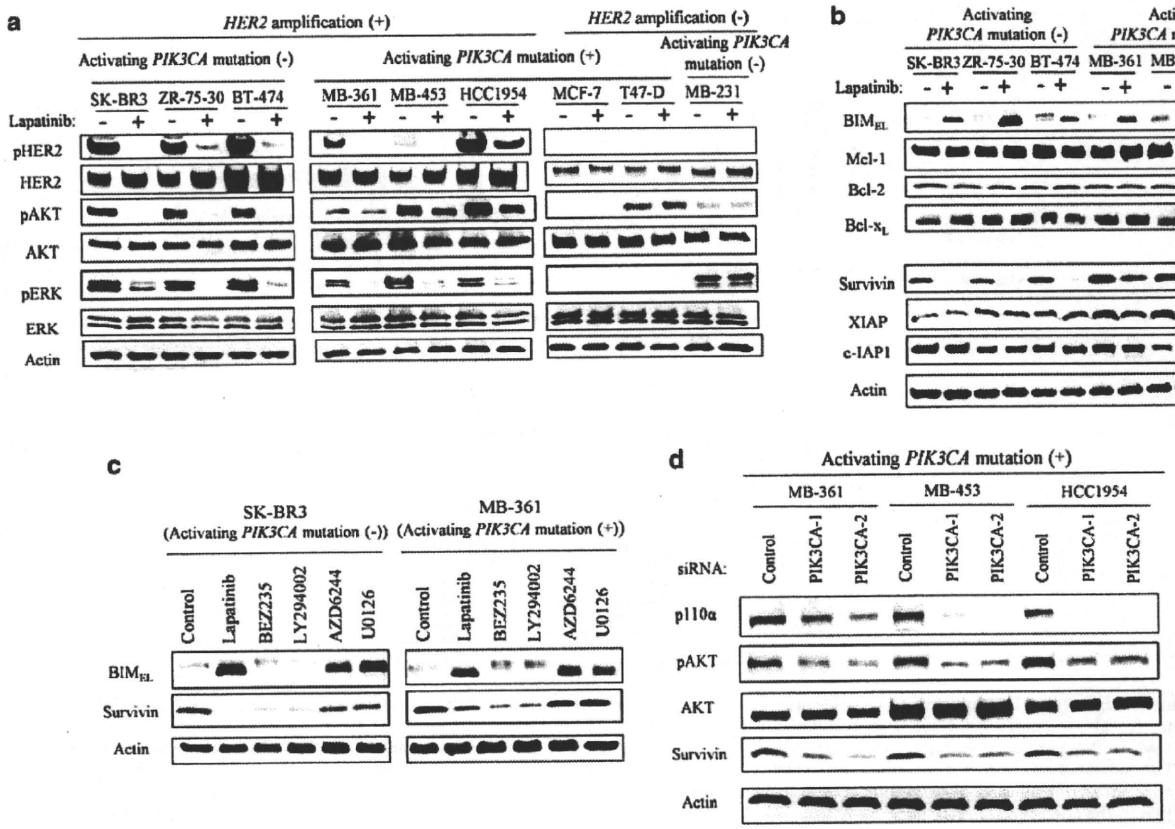

Figure 2 Effects of lapatinib on HER2, AKT and ERK phosphorylation as well as on apoptosis-related protein expression in breast cancer cell lines. (**a**, **b**) The indicated cell lines were incubated with or without lapatinib (1 μM) for 24 h (**a**) or 48 h (**b**), after which cell lysates were prepared and subjected to immunoblot analysis with antibodies to phosphorylated (p) or total forms of HER2, AKT or ERK as well as with those to the indicated apoptosis-related proteins or to β-actin (loading control). The position of the band corresponding to BIM_{EL} is indicated. (**c**) SK-BR3 or MB-361 cells were incubated in the absence (control, 0.1% dimethyl sulfoxide) or presence of lapatinib (1 μM), BEZ235 (0.3 μM), LY294002 (20 μM), AZD6244 (0.3 μM) or U0126 (20 μM) for 48 h, after which cell lysates were prepared and subjected to immunoblot analysis with antibodies to BIM, to survivin or to β-actin. (**d**) The indicated cell lines were transfected with non-specific (control), PIK3CA-1 or PIK3CA-2 siRNAs for 48 h, after which cell lysates were prepared and subjected to immunoblot analysis with antibodies to the indicated proteins.

member of the Bcl-2 family of proteins, in *HER2* amplification-positive cells regardless of the *PIK3CA* mutational status, whereas it had little effect on the expression of other Bcl-2 family members, including Mcl-1, Bcl-2 and Bcl-x_L. Quantitative reverse transcription and PCR analysis showed that lapatinib increased the amount of BIM mRNA in all *HER2* amplification-positive cells in a manner independent of the *PIK3CA* mutational status (Supplementary Figure 1), suggesting that BIM induction by lapatinib is mediated at the transcriptional level. On the other hand, lapatinib downregulated the expression of survivin, a member of the inhibitor of apoptosis protein (IAP) family, in *HER2* amplification-positive cells without an activating *PIK3CA* mutation but not in those with such a mutation. The expression of other IAP family members, including XIAP and c-IAP1, was not substantially affected by lapatinib in any of the cell lines examined.

To identify the signaling pathways responsible for induction of BIM and downregulation of survivin by lapatinib, we examined the effects of specific inhibitors of PI3K (BEZ235 and LY294002) and of the ERK kinase MEK (AZD6244 and U0126). Each of the MEK inhibitors induced BIM expression without affecting the expression of survivin in *HER2* amplification-positive cells regardless of the *PIK3CA* mutational status (Figure 2c), suggesting that expression of BIM is regulated by the MEK-ERK pathway. Conversely, the PI3K inhibitors reduced the abundance of survivin without affecting that of BIM in all cells with *HER2* amplification (Figure 2c). We further examined the effect of depletion of PIK3CA (p110α) by RNA interference (RNAi) on survivin expression in *PIK3CA* mutant cells. Introduction of two independent small interfering RNAs (siRNAs) specific for PIK3CA mRNA (PIK3CA-1 and PIK3CA-2 siRNAs) into *HER2* amplification-positive cells with an activating *PIK3CA* mutation, resulted in a marked decrease in the expression of p110α and a concomitant decrease in the level of AKT phosphorylation. This depletion of p110α was also associated with downregulation of survivin expression in these cell lines (Figure 2d), suggesting that survivin expression was regulated through the PI3K pathway. Together, these data suggested that lapatinib induced BIM expression through inhibition of the MEK-ERK pathway in *HER2* amplification-positive

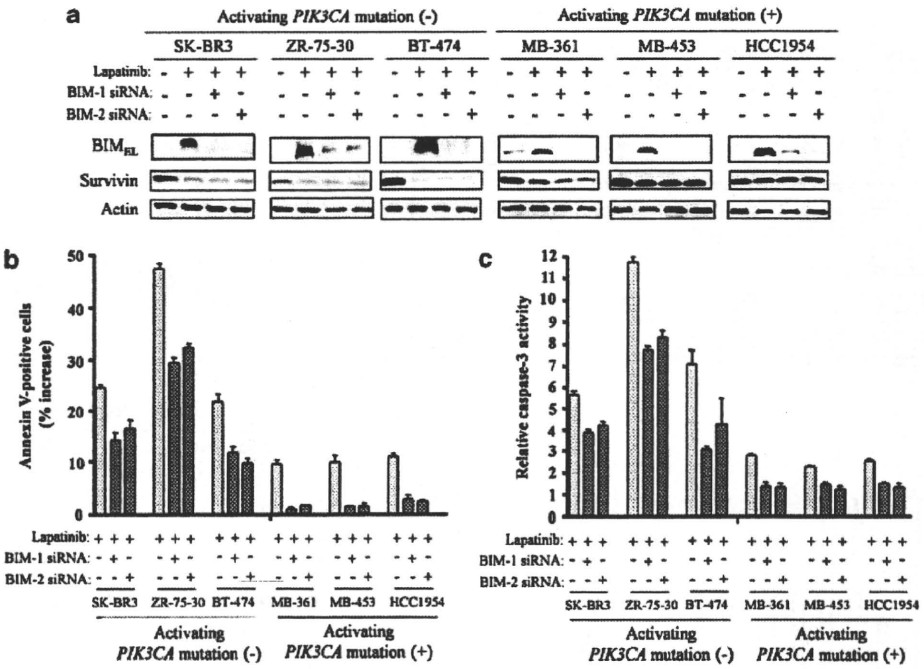

Figure 3 Effect of inhibition of BIM induction on lapatinib-induced apoptosis in *HER2* amplification-positive breast cancer cells with or without an activating *PIK3CA* mutation. (**a**) The indicated cell lines were transfected with BIM-1, BIM-2 or non-specific siRNAs for 24 h and then incubated for 48 h in complete medium with or without lapatinib (1 μM). Cell lysates were then prepared and subjected to immunoblot analysis with antibodies to BIM, to survivin or to β-actin. (**b**) Cells transfected as in a were incubated for 72 h with or without lapatinib (1 μM), and then evaluated for the proportion of apoptotic cells by staining with annexin V and propidium iodide followed by flow cytometry. The percentage increase in the number of apoptotic cells relative to the corresponding value for cells transfected with the control siRNA and incubated without lapatinib is shown. (**c**) Lysates prepared from cells treated as in (**a**) were assayed for caspase-3 activity, which is expressed relative to the corresponding value for cells transfected with the control siRNA and incubated without lapatinib. Data in b and c are means ± s.e. from three independent experiments.

cells with or without an activating *PIK3CA* mutation. On the other hand, lapatinib downregulated survivin expression through inhibition of the PI3K signaling pathway in *HER2* amplification-positive cells without a *PIK3CA* mutation, but it had little effect on survivin expression in cells with such a mutation, likely as a result of activation of the PI3K pathway by the *PIK3CA* mutation.

Effect of inhibition of BIM induction on lapatinib-induced apoptosis in cells with HER2 *amplification*

To investigate the role of BIM induction in lapatinib-induced apoptosis, we transfected *HER2* amplification-positive cells with two independent siRNAs specific for BIM mRNA (BIM-1 and BIM-2 siRNAs). Each BIM siRNA markedly suppressed the lapatinib-induced upregulation of BIM without affecting lapatinib-induced downregulation of survivin (Figure 3a). The annexin V binding assay showed that such transfection resulted in partial inhibition of lapatinib-induced apoptosis in *HER2* amplification-positive cells without an activating *PIK3CA* mutation, whereas lapatinib-induced apoptosis was almost completely inhibited by BIM siRNA in cells with such a mutation (Figure 3b). Similar to the results of the annexin V binding assay, transfection with BIM siRNA resulted in partial inhibition of the lapatinib-induced activation of caspase-3 in cells without a *PIK3CA* mutation, whereas it resulted in almost complete inhibition of this effect of lapatinib in cells with a *PIK3CA* mutation (Figure 3c). The BH3-mimetic ABT737, which binds to anti-apoptotic Bcl-2 family members, including Bcl-2, Bcl-xl and Bcl-w, was shown to enhance apoptosis under conditions of BIM induction (Cragg *et al.*, 2007, 2008; Gong *et al.*, 2007). We therefore examined the effect of the combination of lapatinib and ABT737 on induction of apoptosis in *HER2*-amplified breast cancer cells with or without a *PIK3CA* mutation. We found that ABT737 enhanced lapatinib-induced apoptosis both in HER2-positive cells without a *PIK3CA* mutation, and in those with a *PIK3CA* mutation with an average fold increase of 1.20 and 1.48, respectively ($P<0.05$) (Supplementary Figure 2), supporting a role for BIM induction in lapatinib-induced apoptosis. These data thus indicated that BIM induction contributes to lapatinib-induced apoptosis in cells with *HER2* amplification, but that the extent of this contribution differs according to the mutational status of *PIK3CA*.

Combined effect of lapatinib and BEZ235 on apoptosis in HER2 *amplification-positive cells with an activating* PIK3CA *mutation*

Given that lapatinib manifested only a moderate pro-apoptotic effect in cells with an activating *PIK3CA*

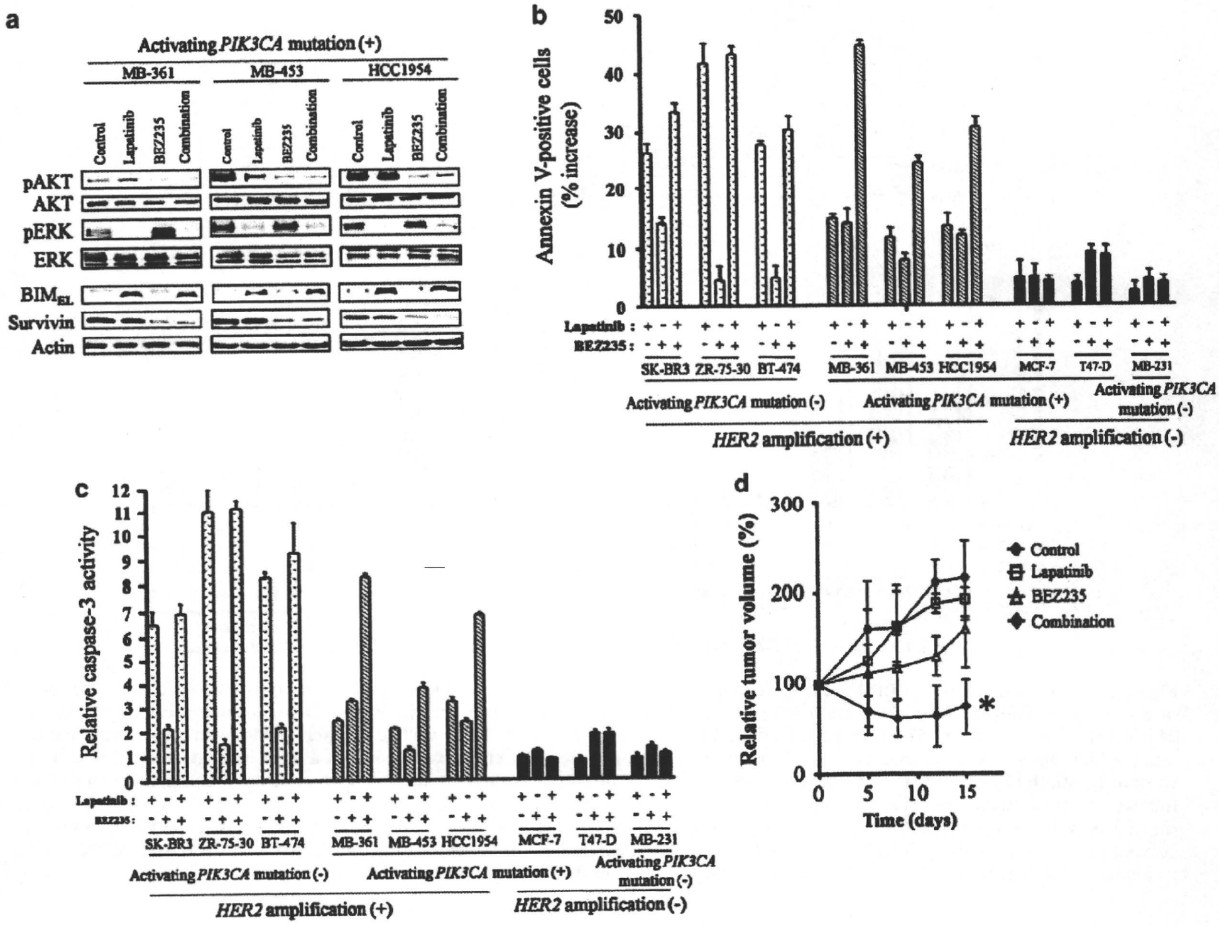

Figure 4 Effects of the combination of BEZ235 and lapatinib in *HER2* amplification-positive cells with an activating *PIK3CA* mutation. (**a**) The indicated cell lines were incubated in the absence (control, 0.1% dimethyl sulfoxide) or presence of lapatinib (1 μM), BEZ235 (0.03 μM) or both agents (combination) for 48 h, after which cell lysates were prepared and subjected to immunoblot analysis with antibodies to the indicated proteins. (**b**) Cells were incubated in the absence or presence of lapatinib (1 μM) or BEZ235 (0.03 μM), as indicated, for 72 h, after which the proportion of apoptotic cells was determined by staining with annexin V and propidium iodide followed by flow cytometry. The percentage increase in the number of apoptotic cells relative to the corresponding value for cells incubated without addition is shown. (**c**) Cells treated as in (**a**) were lysed and assayed for caspase-3 activity, which is expressed relative to the corresponding value for cells incubated without addition. Data in (**b**, **c**) are means ± s.e. from three independent experiments. (**d**) Nude mice with tumor xenografts established by subcutaneous injection of HCC1954 cells were treated daily for 2 weeks with vehicle (control), BEZ235 (15 mg/kg per day), lapatinib (100 mg/kg per day) or the combination of both drugs. Tumor size was determined at the indicated times after treatment onset and is expressed as a percentage of that at time 0. Data are means ± s.e. for six mice per group. $^*P<0.05$ for the combination of BEZ235 and lapatinib versus either BEZ235 or lapatinib alone.

mutation despite the preserved induction of BIM, we hypothesized that insufficient inhibition of the PI3K pathway by lapatinib might be responsible for the limited size of this effect compared with that observed in cells without such a mutation. We therefore examined whether additional inhibition of the PI3K pathway by BEZ235 might enhance the effect of lapatinib on apoptosis in *PIK3CA* mutant cells. Treatment with BEZ235, which was previously shown to inhibit the PI3K pathway in cells expressing activated PIK3CA (Serra *et al*., 2008; Brachmann *et al*., 2009), resulted in marked inhibition of AKT phosphorylation (but not of ERK phosphorylation) in *HER2* amplification-positive cells with an activating *PIK3CA* mutation (Figure 4a). The combination of BEZ235 and lapatinib resulted in inhibition of both AKT and ERK phosphorylation (Figure 4a). Consistent with the notion that regulation of survivin is mediated through the PI3K pathway and that of BIM is mediated through the MEK-ERK pathway, treatment with BEZ235 alone induced downregulation of survivin expression without affecting BIM expression, whereas the combination of BEZ235 and lapatinib elicited both survivin downregulation and BIM upregulation (Figure 4a). The combination of BEZ235 and lapatinib increased the number of apoptotic cells to an extent markedly greater than that apparent with either agent alone in *HER2* amplification-positive cells with a *PIK3CA* mutation, whereas the effect of lapatinib was similar in the absence or presence of BEZ235 in those without a *PIK3CA* mutation or in cells negative for *HER2* amplification (Figure 4b). A similar pattern was observed for the effects of lapatinib and

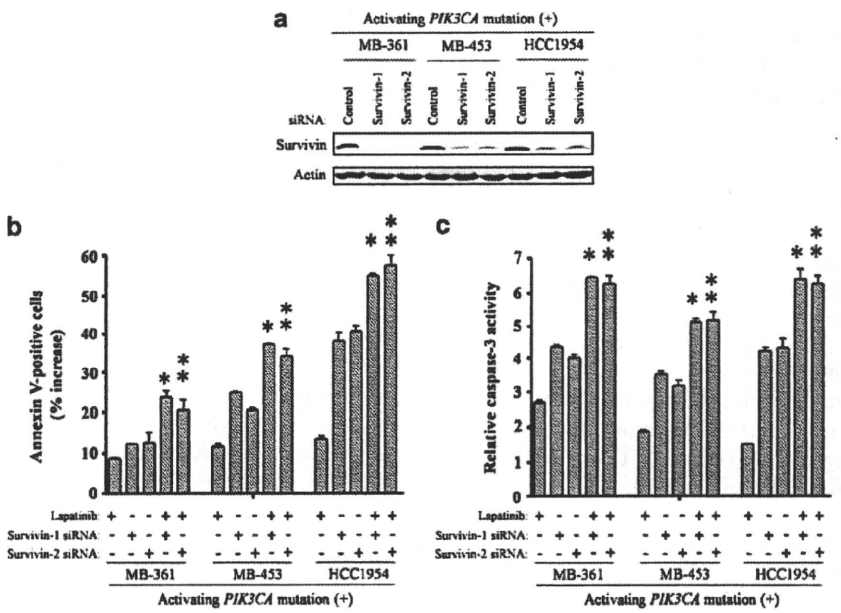

Figure 5 Effect of survivin depletion on apoptosis in *HER2* amplification-positive cells with an activating *PIK3CA* mutation. (**a**) The indicated cell lines were transfected with non-specific (control), survivin-1 or survivin-2 siRNAs for 48 h, after which cell lysates were prepared and subjected to immunoblot analysis with antibodies to survivin or to β-actin. (**b**) Cells transfected as in (**a**) were incubated in complete medium with or without lapatinib (1 μM) for 72 h, after which the proportion of apoptotic cells was determined by staining with annexin V and propidium iodide followed by flow cytometry. The percentage increase in the number of apoptotic cells relative to the corresponding value for cells transfected with the control siRNA and incubated without lapatinib is shown. (**c**) Cells transfected as in (**a**) were incubated with or without lapatinib (1 μM) for 48 h, lysed and assayed for caspase-3 activity, which is expressed relative to the corresponding value for cells transfected with the control siRNA and incubated without lapatinib. Data in (**b**, **c**) are means ± s.e. from three independent experiments. $*P<0.05$ for the combination of lapatinib plus transfection with survivin-1 siRNA versus either treatment alone. $**P<0.05$ for the combination of lapatinib plus transfection with survivin-2 siRNA versus either treatment alone.

BEZ235 on caspase-3 activity (Figure 4c). We further examined the effect of combined treatment with BEZ235 and lapatinib on the growth *in vivo* of *HER2* amplification-positive breast cancer cells with a *PIK3CA* mutation. At the completion of the experiments, tumors treated with either control or lapatinib alone had doubled in size, whereas the combination of lapatinib and BEZ235 maintained tumor regression ($P<0.05$) (Figure 4d), consistent with the combined effect of these agents observed in our *in vitro* experiments. All treatments were well tolerated by the mice, with no signs of toxicity or weight loss during therapy (data not shown). These results thus suggested that effective inhibition of the PI3K pathway and lapatinib treatment cooperate to elicit a substantial level of apoptosis that is accompanied by BIM induction and survivin down-regulation in *HER2* amplification-positive cells with an activating *PIK3CA* mutation.

Combined effect of lapatinib and depletion of survivin on apoptosis in HER2 *amplification-positive cells with an activating* PIK3CA *mutation*

Finally, to investigate the effect of downregulation of survivin expression on apoptosis in *HER2* amplification-positive cells with an activating *PIK3CA* mutation, we depleted such cells of survivin by RNAi (Figure 5a). Each of two independent survivin siRNAs induced apoptosis in these cells, whereas the combination of survivin depletion and lapatinib increased the number of apoptotic cells to an extent significantly greater than that observed with either treatment alone (Figure 5b). These effects on the number of apoptotic cells were confirmed by measurement of caspase-3 activity (Figure 5c). These data thus suggested that down-regulation of survivin itself has a pro-apoptotic effect in cells with a *PIK3CA* mutation, but that survivin depletion and lapatinib cooperate to induce an enhanced level of apoptosis.

Discussion

HER2 amplification is a frequent molecular abnormality in breast cancer, and is associated with a poor outcome and aggressiveness of the disease (Slamon *et al.*, 1987, 1989). Lapatinib, a dual tyrosine kinase inhibitor of EGFR and HER2, shows anti-tumor activity in HER2-overexpressing breast cancer (Geyer *et al.*, 2006; Konecny *et al.*, 2006; Gomez *et al.*, 2008), but the precise mechanism of its anti-tumor effect has remained unclear. We have now investigated the downstream mediators of lapatinib-induced apoptosis in breast cancer cells with *HER2* amplification. BIM is a key pro-apoptotic member of the Bcl-2 family of proteins,

and initiates apoptosis signaling by binding to and antagonizing the function of pro-survival Bcl-2 family members (Chen *et al.*, 2005). Our results indicate that lapatinib induces upregulation of BIM expression in *HER2* amplification-positive cells, and that depletion of BIM by RNAi results in marked inhibition of lapatinib-induced apoptosis in these cells. These data suggest that upregulation of BIM expression contributes to the induction of apoptosis by lapatinib in breast cancer cells with *HER2* amplification. We found that BIM induction by lapatinib occurred in *HER2* amplification-positive cells regardless of *PIK3CA* mutational status and was associated with inhibition of ERK phosphorylation. With the use of specific inhibitors of MEK, we also found that regulation of BIM expression is mediated by the MEK-ERK signaling pathway. These findings are consistent with those of previous studies showing that MEK inhibitors induce BIM expression in B-RAF mutant cells (Cragg *et al.*, 2008), and that inhibition of the MEK-ERK pathway contributes to BIM induction by EGFR tyrosine kinase inhibitors in non-small cell lung cancer (Costa *et al.*, 2007; Cragg *et al.*, 2007; Gong *et al.*, 2007), and that such upregulation of BIM has an essential role in the induction of apoptosis by these agents. We also found that ABT737 enhanced the induction of apoptosis by lapatinib in cells with *HER2* amplification regardless of *PIK3CA* mutational status, further supporting a role for BIM induction in lapatinib-induced apoptosis. To our knowledge, the present study is the first to show that induction of BIM through inhibition of the MEK-ERK pathway is required for lapatinib-induced apoptosis in breast cancer with *HER2* amplification.

Although lapatinib-induced upregulation of BIM expression occurred in a manner independent of *PIK3CA* mutational status, the pro-apoptotic effect of lapatinib was less pronounced in cells with an activating *PIK3CA* mutation than in those without one. Given that such *PIK3CA* mutations result in hyperactivation of the PI3K signaling pathway (Isakoff *et al.*, 2005; Zhao *et al.*, 2005; Berns *et al.*, 2007), we examined whether activation of this pathway was associated with this difference in the extent of apoptosis. Indeed, we found that lapatinib did not inhibit the phosphorylation of AKT in *HER2* amplification-positive cells with an activating *PIK3CA* mutation. We therefore examined the effect of specific inhibitors of the PI3K pathway on lapatinib-induced apoptosis in cells with a *PIK3CA* mutation. Treatment with BEZ235 effectively inhibited AKT phosphorylation, and the combination of BEZ235 and lapatinib thus inhibited both AKT and ERK phosphorylation and had a pro-apoptotic effect that was markedly greater than that observed with either agent alone. Consistent with these *in vitro* experiments, the combination of lapatinib and BEZ235 exhibits an enhanced anti-tumor effect *in vivo* with HER2-positive xenografts with a *PIK3CA* mutation. These results suggest that additional inhibition of the PI3K pathway is required for effective induction of apoptosis by lapatinib in cells with a *PIK3CA* mutation. Lapatinib shows clinical efficacy both alone and in combination with chemotherapeutic agents, but not all patients with *HER2* amplification-positive tumors respond to such treatment (Slamon *et al.*, 1987; Slamon, 1990; Geyer *et al.*, 2006; Di Leo *et al.*, 2008; Gomez *et al.*, 2008). *PIK3CA* mutations have been detected in 20–30% of breast cancer patients with *HER2* amplification (Saal *et al.*, 2005; Stemke-Hale *et al.*, 2008), and our data now suggest that activation of the PI3K signaling pathway associated with the presence of a *PIK3CA* mutation may be responsible, at least in part, for the limited efficacy of lapatinib in patients with tumors positive for both *HER2* amplification and a *PIK3CA* mutation. Similar to the effects of lapatinib, the MEK inhibitor AZD6244 inhibited ERK phosphorylation and increased BIM expression, without affecting AKT phosphorylation or survivin expression, and it cooperated with BEZ235 to induce apoptosis in *HER2* amplification-positive cells with a *PIK3CA* mutation (Supplementary Figure 3). These data thus indicate the importance of simultaneous interruption of the PI3K-survivin and MEK-ERK-BIM pathways for effective induction of apoptosis in such cells. However, the extent of apoptosis induced by AZD6244 alone or in combination with BEZ235 was less pronounced than that induced by lapatinib, suggesting that the anti-tumor effect of lapatinib in these cells is not mediated exclusively through inhibition of MEK-ERK signaling. Further investigation is thus needed to clarify the relationship of *PIK3CA* mutational status to the efficacy of lapatinib. The development of PI3K inhibitors has advanced substantially in recent years, and clinical trials of these agents alone or in combination with other anti-tumor agents are under way. Our study therefore provides a rationale for clinical evaluation of combination therapy with lapatinib and a PI3K inhibitor in breast cancer patients with *HER2* amplification and a *PIK3CA* mutation.

Survivin is essential for proper completion of various stages of cell division, with this protein having been found to contribute to centrosomal function, spindle formation and kinetochore attachment to spindle microtubules (Speliotes *et al.*, 2000; Uren *et al.*, 2000). Survivin is preferentially expressed during the mitotic phase of the cell cycle and is physically associated with the mitotic apparatus. It has also been found to be overexpressed in some tumors, with such overexpression having been associated with a poor clinical outcome (Ambrosini *et al.*, 1997; Tanaka *et al.*, 2000; Altieri, 2003). Like other members of the IAP family such as XIAP and c-IAP1, survivin contains a single BIR (baculoviral IAP repeats) domain. Molecular antagonists of survivin, including anti-sense and siRNA oligonucleotides as well as dominant negative mutants, have been shown to induce apoptosis (Olie *et al.*, 2000; Kanwar *et al.*, 2001), suggestive of an association between survivin and apoptosis. Consistent with these previous findings, we have now shown that depletion of survivin by two independent siRNAs specific for survivin mRNA increased the number of apoptotic cells and the activity of caspase-3 in *HER2* amplification-positive breast cancer cells with a *PIK3CA* mutation. With the use of siRNAs specific for PIK3CA mRNA,

we further showed that survivin expression is regulated by the PI3K signaling pathway, consistent with previous studies linking survivin expression to this signaling pathway (McKenzie *et al.*, 2010; Peirce *et al.*, 2010). Our finding that survivin downregulation through inhibition of PI3K signaling was associated with the induction of apoptosis, is consistent with the key role of this signaling pathway in cell survival. We found that lapatinib downregulated survivin expression in association with the induction of apoptosis in *HER2* amplification-positive cells without an activating *PIK3CA* mutation. In contrast, expression of survivin was not markedly affected by lapatinib in cells harboring such a *PIK3CA* mutation. We therefore examined the effect of inhibition of survivin expression on lapatinib-induced apoptosis in *PIK3CA* mutant cells. In such cells, the combination of survivin depletion by RNAi and lapatinib treatment exhibited a pro-apoptotic effect markedly greater than that observed with either approach alone, suggesting that downregulation of survivin promotes lapatinib-induced apoptosis. We also found that, unlike lapatinib, the PI3K inhibitor BEZ235 induced downregulation of survivin expression in cells with an activating *PIK3CA* mutation, suggesting that this effect contributes, at least in part, to the enhanced level of apoptosis induced by the combination of lapatinib and BEZ235. Insufficient inhibition of the PI3K-survivin pathway may thus account for the smaller pro-apoptotic effect of lapatinib in *HER2* amplification-positive cells with an activating *PIK3CA* mutation compared with that observed in those without such a mutation.

In conclusion, we have shown that both induction of BIM and inhibition of survivin have a role in lapatinib-induced apoptosis in *HER2* amplification-positive breast cancer cells. Moreover, both the PI3K-survivin pathway and the MEK-ERK-BIM pathway contribute independently to the induction of apoptosis in these cells regardless of *PIK3CA* mutational status. Our data thus show that simultaneous interruption of the PI3K-survivin and MEK-ERK-BIM pathways is required for effective induction of apoptosis in breast cancer cells with *HER2* amplification. They further provide a rationale for the development of new therapeutic strategies for patients with breast tumors positive for *HER2* amplification, including those with an activating *PIK3CA* mutation.

Materials and methods

Cell culture and reagents

The human breast cancer cell lines SK-BR3, ZR-75-30, BT-474, MB-361, MB-453, HCC1954, MCF-7, T47-D and MB-231 were obtained from American Type Culture Collection (Manassas, VA, USA). SK-BR3 cells were cultured in McCoy's medium (Invitrogen, Carlsbad, CA, USA) supplemented with 10% fetal bovine serum; BT-474 cells in Dulbecco's modified Eagle's medium (Invitrogen) supplemented with 10% fetal bovine serum; MB-361, MB-453 and MB-231 cells in L15 medium (Invitrogen) supplemented with 10% fetal bovine serum; and the remaining cells in RPMI 1640 medium (Sigma, St Louis, MO, USA) supplemented with 10% fetal bovine serum. All cells were maintained under a humidified atmosphere of 5% CO_2 at 37 °C. Lapatinib was obtained from Sequoia Research Products (Pangbourne, UK), AZD6244 was from ShangHai Biochempartner (Shanghai, China) and LY294002 and U0126 were from Cell Signaling Technology (Danvers, MA, USA). BEZ235 was kindly provided by Novartis (Basel, Switzerland). MB-453 and HCC1954 cells were found to harbor an H1047 hotspot mutation, and MB-361 cells were found to contain an E545K hotspot mutation by sequencing of exons 9 and 20 of *PIK3CA* (Hoeflich *et al.*, 2009; Kataoka *et al.*, 2010; Saal *et al.*, 2005; Samuels *et al.*, 2004). We categorized BT-474 cells as negative for an activating *PIK3CA* mutation for this study on the basis of the demonstrated lack of transforming activity for the K111N mutation and its minimal effect on downstream signaling (Gymnopoulos *et al.*, 2007; Zhang *et al.*, 2008).

Growth inhibition assay in vitro

Cells were plated in 96-well flat-bottomed plates and cultured for 24 h before exposure to various concentrations of lapatinib for 72 h. TetraColor One (5 mM tetrazolium monosodium salt and 0.2 mM 1-methoxy-5-methyl phenazinium methylsulfate; Seikagaku, Tokyo, Japan) was then added to each well, and the cells were incubated for 3 h at 37 °C before measurement of absorbance at 490 nm with a Multiskan Spectrum instrument (Thermo Labsystems, Boston, MA, USA). Absorbance values were expressed as a percentage of that for untreated cells, and the concentration of lapatinib resulting in 50% growth inhibition (IC_{50}) was calculated.

Annexin V binding assay

Binding of annexin V to cells was measured with the use of an Annexin-V-FLUOS Staining Kit (Roche, Basel, Switzerland). Cells were harvested by exposure to trypsin-EDTA, washed with phosphate-buffered saline and centrifuged at 200 *g* for 5 min. The cell pellets were resuspended in 100 µl of Annexin-V-FLUOS labeling solution, incubated for 10–15 min at 15–25 °C and then analyzed for fluorescence with a flow cytometer (FACSCalibur) and Cell Quest software (Becton Dickinson, Franklin Lakes, NJ, USA).

Clonogenicity assay

Cells were seeded in triplicate in six-well plates and cultured for 48 h in the presence of lapatinib (1 µM) or vehicle. They were then cultured in drug-free medium for 14 days, fixed with methanol:acetic acid (10:1, v/v) and stained with crystal violet. The mean percentage cell survival relative to controls was determined from triplicate wells.

Immunoblot analysis

Cells were washed twice with ice-cold phosphate-buffered saline and then lysed in a solution containing 20 mM Tris-HCl (pH 7.5), 150 mM NaCl, 1 mM EDTA, 1% Triton X-100, 2.5 mM sodium pyrophosphate, 1 mM phenylmethylsulfonyl fluoride and leupeptin (1 µg/ml). The protein concentration of cell lysates was determined with a BCA protein assay kit (Thermo Fischer Scientific, Waltham, MA, USA), and equal amounts of protein were subjected to SDS–polyacrylamide gel electrophoresis on a 7.5 or 12% gel (Bio-Rad, Hercules, CA, USA). The separated proteins were transferred to a nitrocellulose membrane, which was then incubated with Blocking One solution (Nacalai Tesque, Kyoto, Japan) for 20 min at room temperature before incubation overnight at 4 °C with primary antibodies. Rabbit polyclonal antibodies to human phosphorylated HER2 (pY1248), to phosphorylated AKT, to

AKT, to BIM, to Mcl-1, to Bcl-2, to Bcl-x_L, to XIAP and to p110α were obtained from Cell Signaling Technology; those to phosphorylated ERK and to ERK were from Santa Cruz Biotechnology (Santa Cruz, CA, USA); those to c-IAP1 were from R&D Systems (Minneapolis, MN, USA); those to HER2 were from Millipore (Billerica, MA, USA); those to survivin were from Novus (Littleton, CO, USA); and those to β-actin were from Sigma. All antibodies were used at a 1:1000 dilution, with the exception of those to β-actin (1:200). The membrane was then washed with phosphate-buffered saline containing 0.05% Tween 20 before incubation for 1 h at room temperature with horseradish peroxidase-conjugated goat antibodies to rabbit immunoglobulin G (Sigma). Immune complexes were finally detected with chemiluminescence reagents (GE Healthcare, Little Chalfont, UK).

Gene silencing

Cells were plated at 50–60% confluence in six-well plates or 25-cm^2 flasks and then incubated for 24 h before transient transfection for the indicated times with siRNAs mixed with the Lipofectamine reagent (Invitrogen). The siRNAs specific for PIK3CA (PIK3CA-1, 5′-UCAACUUCUUCAAGAUG AA-3′; PIK3CA-2, 5′-GUAGAAUGUUUACUACCAA-3′), BIM (BIM-1, 5′-GGAGGGUAUUUUUGAAUAA-3′; BIM-2, 5′-AGGAGGGUAUUUUUGAAUA-3′), or survivin (survivin-1, 5′-GAAGCAGUUUGAAGAAUUA-3′; survivin-2, 5′-AGAAGCAGUUUGAAGAAUU-3′) mRNAs as well as non-specific (control) siRNAs were obtained from Nippon EGT (Toyama, Japan).

Assay of caspase-3 activity

The activity of caspase-3 in cell lysates was measured with the use of a CCP32/Caspase-3 Fluometric Protease Assay Kit (MBL, Woburn, MA, USA). Fluorescence attributable to cleavage of the Asp–Glu–Val–Asp–7-amino-4-trifluoromethyl coumarin (DEVD-AFC) substrate was measured at excitation and emission wavelengths of 390 and 460 nm, respectively.

Growth inhibition assay in vivo

All animal studies were done with the Recommendations for Handling of Laboratory Animals for biochemical Research compiled by the Committee on Safety and Ethical Handling Regulations for Laboratory Animal Experiments, Kinki University. Cubic fragments of tumor tissue (~2 by 2 by 2 mm) formed by HCC1954 cells were implanted subcutaneously into the axilla of 5–6-week-old male athymic nude mice. When their tumors became palpable, mice were divided in to four groups and treated with vehicle, BEZ235 alone, lapatinib alone and the combination of BEZ235 and lapatinib. Each treatment group contained six mice. BEZ235 and lapatinib were administered by oral gavage daily for 14 days; control animals received a 0.5% (w/v) aqueous solution of hydroxypropylmethylcellulose as vehicle. Tumor volume was determined from caliper measurements of tumor length (L) and width (W) according to the formula $LW^2/2$. Both tumor size and body weight were measured twice per week.

Statistical analysis

Quantitative data from *in vitro* experiments are presented as means ± s.e. from three independent experiments, and were analyzed with the unpaired two-tailed Student's t-test. *In vivo* data are presented as means ± s.e. from six mice and were analyzed by the unpaired two-tailed Student's t-test. A P-value of <0.05 was considered statistically significant.

Conflict of interest

The authors declare no conflict of interest.

Acknowledgements

We thank E Hatashita, K Kuwata, and H Yamaguchi for technical assistance.

References

Altieri DC. (2003). Validating survivin as a cancer therapeutic target. *Nat Rev Cancer* **3**: 46–54.

Ambrosini G, Adida C, Altieri DC. (1997). A novel anti-apoptosis gene, survivin, expressed in cancer and lymphoma. *Nat Med* **3**: 917–921.

Berns K, Horlings HM, Hennessy BT, Madiredjo M, Hijmans EM, Beelen K *et al.* (2007). A functional genetic approach identifies the PI3K pathway as a major determinant of trastuzumab resistance in breast cancer. *Cancer Cell* **12**: 395–402.

Brachmann SM, Hofmann I, Schnell C, Fritsch C, Wee S, Lane H *et al.* (2009). Specific apoptosis induction by the dual PI3K/mTor inhibitor NVP-BEZ235 in HER2 amplified and PIK3CA mutant breast cancer cells. *Proc Natl Acad Sci USA* **106**: 22299–22304.

Burris III HA, Taylor CW, Jones SF, Koch KM, Versola MJ, Arya N *et al.* (2009). A phase I and pharmacokinetic study of oral lapatinib administered once or twice daily in patients with solid malignancies. *Clin Cancer Res* **15**: 6702–6708.

Chen L, Willis SN, Wei A, Smith BJ, Fletcher JI, Hinds MG *et al.* (2005). Differential targeting of prosurvival Bcl-2 proteins by their BH3-only ligands allows complementary apoptotic function. *Mol Cell* **17**: 393–403.

Costa DB, Halmos B, Kumar A, Schumer ST, Huberman MS, Boggon TJ *et al.* (2007). BIM mediates EGFR tyrosine kinase inhibitor-induced apoptosis in lung cancers with oncogenic EGFR mutations. *PLoS Med* **4**: 1669–1679; discussion 1680.

Cragg MS, Jansen ES, Cook M, Harris C, Strasser A, Scott CL. (2008). Treatment of B-RAF mutant human tumor cells with a MEK inhibitor requires Bim and is enhanced by a BH3 mimetic. *J Clin Invest* **118**: 3651–3659.

Cragg MS, Kuroda J, Puthalakath H, Huang DC, Strasser A. (2007). Gefitinib-induced killing of NSCLC cell lines expressing mutant EGFR requires BIM and can be enhanced by BH3 mimetics. *PLoS Med* **4**: 1681–1689; discussion 1690.

Di Leo A, Gomez HL, Aziz Z, Zvirbule Z, Bines J, Arbushites MC *et al.* (2008). Phase III, double-blind, randomized study comparing lapatinib plus paclitaxel with placebo plus paclitaxel as first-line treatment for metastatic breast cancer. *J Clin Oncol* **26**: 5544–5552.

Eichhorn PJ, Gili M, Scaltriti M, Serra V, Guzman M, Nijkamp W *et al.* (2008). Phosphatidylinositol 3-kinase hyperactivation results in lapatinib resistance that is reversed by the mTOR/phosphatidylinositol 3-kinase inhibitor NVP-BEZ235. *Cancer Res* **68**: 9221–9230.

Geyer CE, Forster J, Lindquist D, Chan S, Romieu CG, Pienkowski T *et al.* (2006). Lapatinib plus capecitabine for HER2-positive advanced breast cancer. *N Engl J Med* **355**: 2733–2743.

Gomez HL, Doval DC, Chavez MA, Ang PC, Aziz Z, Nag S *et al.* (2008). Efficacy and safety of lapatinib as first-line therapy for ErbB2-amplified locally advanced or metastatic breast cancer. *J Clin Oncol* **26**: 2999–3005.

Gong Y, Somwar R, Politi K, Balak M, Chmielecki J, Jiang X *et al.* (2007). Induction of BIM is essential for apoptosis triggered by EGFR kinase inhibitors in mutant EGFR-dependent lung adenocarcinomas. *PLoS Med* **4**: e294.

Gymnopoulos M, Elsliger MA, Vogt PK. (2007). Rare cancer-specific mutations in PIK3CA show gain of function. *Proc Natl Acad Sci USA* **104**: 5569–5574.

Hoeflich KP, O'Brien C, Boyd Z, Cavet G, Guerrero S, Jung K *et al.* (2009). *in vivo* antitumor activity of MEK and phosphatidylinositol 3-kinase inhibitors in basal-like breast cancer models. *Clin Cancer Res* **15**: 4649–4664.

Isakoff SJ, Engelman JA, Irie HY, Luo J, Brachmann SM, Pearline RV *et al.* (2005). Breast cancer-associated PIK3CA mutations are oncogenic in mammary epithelial cells. *Cancer Res* **65**: 10992–11000.

Kanwar JR, Shen WP, Kanwar RK, Berg RW, Krissansen GW. (2001). Effects of survivin antagonists on growth of established tumors and B7-1 immunogene therapy. *J Natl Cancer Inst* **93**: 1541–1552.

Kataoka Y, Mukohara T, Shimada H, Saijo N, Hirai M, Minami H. (2010). Association between gain-of-function mutations in PIK3CA and resistance to HER2-targeted agents in HER2-amplified breast cancer cell lines. *Ann Oncol* **21**: 255–262.

Konecny GE, Pegram MD, Venkatesan N, Finn R, Yang G, Rahmeh M *et al.* (2006). Activity of the dual kinase inhibitor lapatinib (GW572016) against HER-2-overexpressing and trastuzumab-treated breast cancer cells. *Cancer Res* **66**: 1630–1639.

LoRusso PM, Jones SF, Koch KM, Arya N, Fleming RA, Loftiss J *et al.* (2008). Phase I and pharmacokinetic study of lapatinib and docetaxel in patients with advanced cancer. *J Clin Oncol* **26**: 3051–3056.

McKenzie JA, Liu T, Goodson AG, Grossman D.. (2010). Survivin enhances motility of melanoma cells by supporting Akt activation and {alpha}5 inte. *Cancer Res* **70**: 7927–7937.

Olie RA, Simoes-Wust AP, Baumann B, Leech SH, Fabbro D, Stahel RA *et al.* (2000). A novel antisense oligonucleotide targeting survivin expression induces apoptosis and sensitizes lung cancer cells to chemotherapy. *Cancer Res* **60**: 2805–2809.

Peirce SK, Findley HW, Prince C, Dasgupta A, Cooper T, Durden DL. (2010). The PI-3 kinase-Akt-MDM2-survivin signaling axis in high-risk neuroblastoma: a target for PI-3 kinase inhibitor intervention. *Cancer Chemother Pharmacol* (e-pub ahead of print 24 October 2010; DOI:10.1007/s00280-1010-1486-7).

Saal LH, Holm K, Maurer M, Memeo L, Su T, Wang X *et al.* (2005). PIK3CA mutations correlate with hormone receptors, node metastasis, and ERBB2, and are mutually exclusive with PTEN loss in human breast carcinoma. *Cancer Res* **65**: 2554–2559.

Samuels Y, Wang Z, Bardelli A, Silliman N, Ptak J, Szabo S *et al.* (2004). High frequency of mutations of the PIK3CA gene in human cancers. *Science* **304**: 554.

Serra V, Markman B, Scaltriti M, Eichhorn PJ, Valero V, Guzman M *et al.* (2008). NVP-BEZ235, a dual PI3K/mTOR inhibitor, prevents PI3K signaling and inhibits the growth of cancer cells with activating PI3K mutations. *Cancer Res* **68**: 8022–8030.

Slamon DJ. (1990). Studies of the HER-2/neu proto-oncogene in human breast cancer. *Cancer Invest* **8**: 253.

Slamon DJ, Clark GM, Wong SG, Levin WJ, Ullrich A, McGuire WL. (1987). Human breast cancer: correlation of relapse and survival with amplification of the HER-2/neu oncogene. *Science* **235**: 177–182.

Slamon DJ, Godolphin W, Jones LA, Holt JA, Wong SG, Keith DE *et al.* (1989). Studies of the HER-2/neu proto-oncogene in human breast and ovarian cancer. *Science* **244**: 707–712.

Speliotes EK, Uren A, Vaux D, Horvitz HR. (2000). The survivin-like C. elegans BIR-1 protein acts with the Aurora-like kinase AIR-2 to affect chromosomes and the spindle midzone. *Mol Cell* **6**: 211–223.

Stemke-Hale K, Gonzalez-Angulo AM, Lluch A, Neve RM, Kuo WL, Davies M *et al.* (2008). An integrative genomic and proteomic analysis of PIK3CA, PTEN, and AKT mutations in breast cancer. *Cancer Res* **68**: 6084–6091.

Tanaka K, Iwamoto S, Gon G, Nohara T, Iwamoto M, Tanigawa N. (2000). Expression of survivin and its relationship to loss of apoptosis in breast carcinomas. *Clin Cancer Res* **6**: 127–134.

Toi M, Iwata H, Fujiwara Y, Ito Y, Nakamura S, Tokuda Y *et al.* (2009). Lapatinib monotherapy in patients with relapsed, advanced, or metastatic breast cancer: efficacy, safety, and biomarker results from Japanese patients phase II studies. *Br J Cancer* **101**: 1676–1682.

Uren AG, Wong L, Pakusch M, Fowler KJ, Burrows FJ, Vaux DL *et al.* (2000). Survivin and the inner centromere protein INCENP show similar cell-cycle localization and gene knockout phenotype. *Curr Biol* **10**: 1319–1328.

Zhang H, Liu G, Dziubinski M, Yang Z, Ethier SP, Wu G. (2008). Comprehensive analysis of oncogenic effects of PIK3CA mutations in human mammary epithelial cells. *Breast Cancer Res Treat* **112**: 217–227.

Zhao JJ, Liu Z, Wang L, Shin E, Loda MF, Roberts TM. (2005). The oncogenic properties of mutant p110alpha and p110beta phosphatidylinositol 3-kinases in human mammary epithelial cells. *Proc Natl Acad Sci USA* **102**: 18443–18448.

Supplementary Information accompanies the paper on the Oncogene website (http://www.nature.com/onc)

Lung Cancer xxx (2011) xxx–xxx

Contents lists available at ScienceDirect

Lung Cancer

journal homepage: www.elsevier.com/locate/lungcan

Duration of prior gefitinib treatment predicts survival potential in patients with lung adenocarcinoma receiving subsequent erlotinib

Kazuhiro Asami [a,*], Masaaki Kawahara [b], Shinji Atagi [a], Tomoya Kawaguchi [a], Kyoichi Okishio [a]

[a] Kinki-chuo Chest Medical Center, 1180 Nagasone-cho, Kita-ku, Sakai City, Osaka 591-8555, Japan
[b] Otemae Hospital, 1-5-34 Otemae, Chuo-ku, Osaka, Japan

ARTICLE INFO

Article history:
Received 9 August 2010
Received in revised form 19 October 2010
Accepted 18 December 2010

Keywords:
Gefitinib
Erlotinib
EGFR mutation
Resistance to EGFR-TKIs
Time to progression of gefitinib

ABSTRACT

Purpose: We investigated survival potential in patients receiving erlotinib after failure of gefitinib, focusing on response and time to progression (TTP) with gefitinib.
Methods: We retrospectively reviewed lung adenocarcinoma patients who received erlotinib after experiencing progression with gefitinib. Our primary objective was to evaluate the prognostic significance of erlotinib therapy.
Results: A total 42 lung adenocarcinoma patients were included in this study. Overall disease control rate was 59.5% (partial response [PR], 2.4%; stable disease [SD], 57.1%). Median overall survival was 7.1 months, and median progression-free survival was 3.4 months. The number of patients who achieved PR and non-PR (SD+ progressive disease [PD]) with gefitinib were 22 (52%) and 20 (48%), respectively. Patients with PR for gefitinib showed significantly longer survival times than those with non-PR (9.2 vs. 4.7 months; $p = 0.014$). In particular, among PR patients, those with TTP <12 months on gefitinib showed significantly longer survival times than those with TTP ≥12 months (10.3 vs. 6.4 months; $p = 0.04$).
Conclusions: Erlotinib may exert survival benefit for lung adenocarcinoma patients with less than 12 months of TTP of prior gefitinib who achieved PR for gefitinib.

1. Introduction

Gefitinib and erlotinib are oral epidermal growth factor receptor tyrosine kinase inhibitors (EGFR-TKIs). Gefitinib has been reported to be effective in limited populations such as never smokers, Asians, and patients with adenocarcinoma, and is particularly effective in patients with EGFR mutations [1–3]. Erlotinib, which has a similar quinazoline frame to gefitinib, is the first EGFR-TKI shown to provide survival benefit in patients with non-small cell lung cancer (NSCLC) [4]: the BR.21 trial revealed significantly longer survival times among patients who received erlotinib compared with a placebo group [4]. In addition, these two EGFR-TKIs have been found to occasionally induce a particularly significant response in EGFR-mutant patients. However, despite this documented efficacy, most cancer clones acquire resistance to these particular compounds over time [5].

Previous studies have demonstrated that amplified MET oncogene and secondary EGFR T790M mutations are most commonly responsible for resistance to gefitinib and erlotinib [6,7]. Indeed, several previous studies showed that secondary EGFR T790M mutation and MET amplification occurred in nearly half and 20% of lung cancer specimens that had become resistant to EGFR-TKIs, respectively [8–11]. In addition, the majority of patients who showed secondary resistance had EGFR mutations such as exon 19 deletion mutations or L858R point mutation, which have been found to be sensitive to EGFR-TKIs [12,13].

Several reports have demonstrated clinical benefits when administering erlotinib to NSCLC patients following failure of gefitinib [14–18]; in contrast, one previous report has suggested that no erlotinib-derived clinical benefit can be expected in patients who failed gefitinib [19]. However, reports thus far have all had small sample sizes, and clear findings regarding efficacy of erlotinib in patients who failed gefitinib have yet to be obtained. Consequently, whether or not erlotinib is useful in these patients remains controversial.

We hypothesize that tumor clones may require exposure to gefitinib treatment with a positive response for a specific duration to acquire secondary common resistance to EGFR-TKIs. Even if a patient experiences tumor progression on gefitinib therapy, subsequent erlotinib therapy may nevertheless still be able to inhibit progression, provided the tumor clones did not acquire secondary resistance. As such, in positive-responder patients with confirmed progression within a specific duration of gefitinib treatment, some tumor clones may remain sensitive to erlotinib, and therefore these patients may still experience survival benefit with erlotinib treatment.

* Corresponding author. Tel.: +81 72 252 3021; fax: +81 72 251 1372.
E-mail address: kazu.taizo@nifty.com (K. Asami).

0169-5002/$ – see front matter © 2011 Elsevier Ireland Ltd. All rights reserved.
doi:10.1016/j.lungcan.2010.12.014

Here, we conducted a retrospective study primarily aimed at assessing overall survival (OS) of patients who received erlotinib therapy after failure with gefitinib. We also attempted to characterize the clinical features of patients who benefited from erlotinib treatment.

2. Patients and methods

We retrospectively reviewed records for patients with histopathologically diagnosed lung adenocarcinoma who received erlotinib after experiencing progression on gefitinib at Kinki-chuo Chest Medical Center between December 2008 and October 2009. Responses were evaluated based on patient records and radiographic studies, such as chest roentgenograms and computed tomographic (CT) and magnetic resonance imaging (MRI) scans. We examined EGFR mutation status using the PCR-invader method with paraffin sections of biopsy specimens from patients.

Time to progression (TTP) with gefitinib was defined as the period from initiation of gefitinib therapy to the date when disease progression was confirmed. Overall survival was defined as the period from initiation of erlotinib therapy to the date of death or last follow-up. Disease control rate (DCR) was defined as complete response (CR) plus partial response (PR) plus stable disease (SD). Evaluation of response to gefitinib and erlotinib therapy by CT scan was performed according to the response evaluation criteria in solid tumors (RECIST). Stable disease plus progressive disease (PD) with prior gefitinib treatment was defined as "non-PR."

Categorical outcomes, including DCRs, were compared using the χ^2 test, and survival distribution was estimating using the Kaplan–Meier method. Overall survival and progression-free survival (PFS) were compared with regard to demographic factors such as gender, performance status, EGFR mutation status, response to gefitinib, TTP with gefitinib, and toxicity grade of skin rash, which may be associated with survival, using the log-rank test. Values were considered statistically significant for $p < 0.05$. A multivariate Cox-proportional-hazards model was used to determine the clinical variables which influenced OS. Statistical analyses were carried out using SPSS software ver. 11.0 for Windows (IBM, Chicago, IL, USA).

3. Results

3.1. Patient characteristics

Forty-two patients with lung adenocarcinoma were reviewed in the present study. All patients became refractory to gefitinib during the course of treatment and were subsequently switched to erlotinib therapy. Patient characteristics are described in detail in Table 1. Thirty patients (71%) had received 1 or 2 regimens before initiation of erlotinib and 2 (7%) had received gefitinib as first-line treatment.

Table 1
Patient characteristics.

	Number (%)
Median age, years (range)	65 (31–85)
Sex	
Male	13 (31)
Female	29 (69)
Smoking history	
Never	28 (67)
Former/current	14 (33)
ECOG score	
0–1	24 (57)
2–4	18 (43)
Cancer stage	
IIIB	8 (19)
IV	34 (81)
Number of previous treatments with erlotinib	
1–2	30[a] (71)
3≤	12 (29)
EGFR mutation	
Exon 19 deletion mutation	14 (33)
L858R	14 (33)
Exon 18 point mutation	1 (2)
Wild	13 (32)
TTP with gefitinib treatment, months (range)	8.1 (0.9–40.7)
<12	29 (69)
≤12	13 (31)
Response to gefitinib	
CR	0 (0)
PR	22 (53)
SD	17 (40)
PD	3 (7)

EGFR, epidermal growth factor receptor; TTP, time to progression; CR, complete response; PR, partial response; SD, stable disease; PD, progressive disease; ECOG, Eastern Cooperative Oncology Group.
[a] Two patients received gefitinib as first-line treatment.

EGFR mutations were detected in 29 (69%) patients: 14 (33%) had exon 19 deletions, 14 (33%) had L858R mutations, and 1 (2%) had an exon 18 point mutation. The median TTP with gefitinib treatment was 8.1 months. Thirteen (31%) patients had TTPs of 12 months or more, while 29 (69%) had TTPs of less than 12 months. Twenty-two (53%) patients receiving gefitinib achieved PR, and 17 (40%) achieved SD. None achieved CR while receiving gefitinib therapy. The response rate (RR) and DCR for gefitinib were 53% (22 of 42 patients) and 93% (39 of 42 patients), respectively. Of the 22 patients who achieved PR with gefitinib, 19 (86%) were found to have EGFR mutations. Of the 20 patients who had SD or PD (non-PR)

Table 2
Response to erlotinib according to the response to prior gefitinib and EGFR mutation status.

EGFR mutation		Response to gefitinib					
		PR ($n=22$)		Non-PR[a] ($n=20$)			
				SD ($n=17$)		PD ($n=3$)	
		Positive, n (%)	Negative[b], n (%)	Positive, n (%)	Negative, n (%)	Positive, n (%)	Negative, n (%)
Response to erlotinib	PR ($N=1$)	1 (4.5)	0 (0)	0 (0)	0 (0)	0 (0)	0 (0)
	SD ($N=24$)	14 (64)	1 (4.5)	3 (18)	5 (29)	0 (0)	1 (33)
	PD ($N=17$)	4 (18)	2 (9)	6 (35)	3 (18)	1 (33)	1 (33)

EGFR, epidermal growth factor receptor; PR, partial response; SD, stable disease; PD, progressive disease. Overall disease control rate (PR+SD) was 73% (EGFR mutation-positive: 15/22 [68%], EGFR mutation-negative: 1/22 [5%]) among patients who achieved PR with gefitinib and 45% (EGFR mutation-positive: 3/20 [15%], EGFR mutation-negative: 6/20 [30%]) among patients with non-PR (SD + PD for gefitinib) with gefitinib treatment. Overall disease control rate was 62% (PR for gefitinib: 15/29 [52%], non-PR for gefitinib: 3/29 [10%]) in EGFR mutation-positive patients and 54% (PR for gefitinib: 1/13 [8%], non-PR for gefitinib: 6/13 [46%]) in EGFR mutation-negative patients.
[a] Defined as SD plus PD with prior gefitinib therapy.
[b] EGFR wild-type.

Please cite this article in press as: Asami K, et al. Duration of prior gefitinib treatment predicts survival potential in patients with lung adenocarcinoma receiving subsequent erlotinib. Lung Cancer (2011), doi:10.1016/j.lungcan.2010.12.014

Table 3
Response to erlotinib stratified by TTP with prior gefitinib treatment.

(A) TTP with gefitinib <12 months				
Response to gefitinib		TTP with gefitinib (months) <12 (n = 29)		
		PR (n = 11) n (%)	Non-PR (n = 18)	
			SD (n = 15) n (%)	PD (n = 3) n (%)
Response to erlotinib	PR (n = 1)	1[b] (9)	0 (0)	0 (0)
	SD (n = 17)	8[a,b] (73)	8[a] (44)	1 (6)
	PD (n = 11)	2 (18)	7 (39)	2 (11)
B. TTP with gefitinib ≥ 12 months				
Response to gefitinib		TTP with gefitinib (months) ≥12 (n = 13)		
		PR (n = 11) n (%)	Non-PR (n = 2)	
			SD (N = 2) n (%)	PD (N = 0) n (%)
Response to erlotinib	PR (n = 0)	0 (0)	0 (0)	0 (0)
	SD (n = 7)	7 (64)	0 (0)	0 (0)
	PD (n = 6)	4 (36)	2 (100)	0 (0)

EGFR, epidermal growth factor receptor; PR, partial response; SD, stable disease; PD, progressive disease; TTP, time to progression. Overall disease control rate was 62% (PR for gefitinib: 9/29 [31%], non-PR for gefitinib: 9/29 [31%]) in patients with TTP of gefitinib <12 months. Overall disease control rate was 54% (PR for gefitinib: 7/13 [54%], non-PR for gefitinib: 0/13 [0%]) in patients with TTP of gefitinib ≥12 months.

[a] Ten patients showed improvement of target lesions, but not to PR standards. Seven and three patients achieved PR and SD, respectively, with gefitinib treatment.

[b] A second biopsy from progression lesions was performed in three patients (one had PR and 2 had SD with erlotinib) who achieved PR with gefitinib. Exon 19 deletion mutations which were the same pattern as detected in first biopsy specimen for primary diagnosis of NSCLC were identified, whereas EGFR T790M mutation, which endowed secondary common resistance to EGFR-TKIs, was not identified in those biopsy specimens.

with gefitinib, EGFR mutations were detected in 10 (50%). Among patients with EGFR mutations, only one showed PD with gefitinib therapy, and RR and DCR in this group were 66% (19 of 29) and 97% (28 of 29), respectively.

3.2. Response

On erlotinib therapy, 1 of 42 patients achieved PR, and 24 had SD. No patients achieved CR with erlotinib. Overall RR and DCR for erlotinib were 2.4% (one of 42) and 59.5% (25 of 42), respectively.

Response to erlotinib categorized by response to prior gefitinib duration and EGFR mutation status is described in Table 2. Among patients who achieved PR with gefitinib, one achieved PR and 15 patients achieved SD with erlotinib therapy. Patients who achieved PR with gefitinib showed higher DCRs with erlotinib than patients who had non-PR with gefitinib (16 [73%] of 22 vs. 9 [45%] of 20), albeit without statistical significance ($p = 0.07$). In addition, EGFR mutation status was not found to be associated with response to erlotinib; in terms of DCR, no significant difference was noted between EGFR-mutant patients (18/29) and EGFR non-mutant patients group (7/13) (62% vs. 54%, $p = 0.616$).

Time to progression with prior administration of gefitinib was not found to be associated with achieving a response with subsequent erlotinib. Details regarding response to erlotinib categorized by TTP with gefitinib are shown in Table 3. DCR among patients experiencing progression after less than 12 months of gefitinib therapy was 18/29 (62%). In contrast, DCR among patients with TTPs of 12 months or more was 7/13 (54%). No statistical significant difference in DCR was noted between these two groups according to TTP with prior administration of gefitinib ($p = 0.62$). Of the 24 patients who achieved SD with erlotinib therapy, 10 showed improvement in target lesions which had been exacerbated during gefitinib treatment; all 10 were EGFR-mutant patients (4 L858R, 5 exon 19 deletion mutations, and 1 exon 18 point mutation), and TTPs with gefitinib were all less than 12 months. Of the two patients who received gefitinib as first-line treatment, one had an EGFR L858R mutation and showed responses to gefitinib and subsequent erlotinib of PR and SD, respectively. While this particular patient showed a relatively long TTP (39.5 months) with gefitinib, disease progression was confirmed 4 months after initiation of erlotinib therapy, and OS was 58.6 months. The other patient who received gefitinib as first-line treatment had EGFR-wild type, and responses to both gefitinib and subsequent erlotinib treatment were PD. TTP and OS in this patient were 3 and 7.4 months, respectively.

A second biopsy of the progressed lesions was performed in three patients after gefitinib therapy failed. While exon 19 deletion mutations of the same pattern as noted in the first biopsy specimen for primary diagnosis were also detected on this second biopsy, we noted no EGFR T790M mutations. Of note, however, was the fact that imaging findings for lesions after erlotinib therapy were improved on the second biopsy (Table 3).

3.3. Survival

Median OS and median progression-free survival (PFS) were 7.1 months (95% confidence interval [CI]: 4.4–9.8 months) and 3.4 months (95% CI: 1.1–5.7 months), respectively (Fig. 1). Multivariate analysis of prognostic factors was performed using a Cox proportional hazards model to determine which clinical variables were most strongly associated with OS (Table 4). Response to gefitinib

Table 4
Multivariate analysis of prognostic variables for OS by use of a Cox proportional-hazards model.

	Multivariate analysis		
	p[a]	Hazard ratio	95% CI
Sex	0.51	1.35	0.55–3.31
ECOG score	0.19	0.58	0.25–1.31
EGFR mutation	0.78	1.13	0.48–2.70
Response to gefitinib	0.005	0.23	0.80–0.64
TTP of gefitinib	0.05	0.34	0.12–1.01
Grade of skin rash	0.29	0.64	0.27–1.47

EGFR, epidermal growth factor receptor; TTP, time to progression; CI, confidence interval; ECOG, Eastern Cooperative Oncology Group; PR, partial response. Response to gefitinib was the only independent prognostic factor. TTP with gefitinib showed borderline significance. Variables were compared as paired categories: sex (female vs. male), ECOG score (0–1 vs. 2–4), response to gefitinib (PR vs. non-PR), TTP of gefitinib (<12 months vs. ≥12 months), grade of skin rash (3 vs. 1–2).

[a] $p < 0.05$ was considered significant.

Please cite this article in press as: Asami K, et al. Duration of prior gefitinib treatment predicts survival potential in patients with lung adenocarcinoma receiving subsequent erlotinib. Lung Cancer (2011), doi:10.1016/j.lungcan.2010.12.014